Norwegian University of Life Sciences
Faculty of Environmental Science and
Technology
Department of Ecology and Natural Resource
Management

Validating Kinematic Wake Models in Complex Terrain Using CFD

Fredrik Seim

Acknowledgements

Abstract

Due to spatial and economic constraints and the limited number of suitable sites, wind turbines are clustered in wind farms. A turbine operating downwind of another turbine will stand in the wake of the first turbine, encountering reduced wind speeds, higher turbulence and will most likely generate less energy. In order to keep wake losses at a minimum, wind farm designers rely on wake models to optimize the turbine layout. Kinematic wake models are often preferred due to their low calculation time. Measurements from Nygårdsfjellet wind farm located in northern Norway have been used in an attempt to validate three kinematic wake models, namely the Jensen-, Larsen- and Ishihara model. Assisted by the commercial WindSim software, which is based on computational fluid dynamics (CFD), the accuracy of the three models were tested in eight single-wake cases with regard to several key aspects. Due to the complex terrain, a range of issues complicated the validation procedure. The Ishihara model was found to overestimate the normalized power deficit in all cases. The Jensen model also overestimated the peak power deficit, but not to the same extent. Finally, the Larsen model correlated well with the measured data. At the wake centerline, the Larsen model was by far the most accurate, with a mean absolute error of 7 %. The Jensen- and Ishihara model had a mean absolute error of 21 and 34 % respectively. The Larsen model widely overestimated the wake width in all cases, but with an almost constant offset. Both the Jensen- and Ishihara model agreed well with the observed wake width. For the energy loss in the wake, the Larsen model performed best for the three investigated wake cases with a mean absolute error of 29 %, although all the three wake models showed a varying performance with a tendency to underestimate the energy loss. However, after employing a procedure to correct for simulation errors, the Ishihara model performed best with a mean absolute error for 10 %. The actuator disc approach accurately simulated the velocity deficit in the wake, all though a slight overestimation of the wind velocity was present. Overall, findings indicated that the Larsen model performed best, although it constantly overestimated the wake width and showed tendencies to underestimate the energy loss in the wake. But no clear-cut conclusion can be drawn on which model is the most accurate due to both unsatisfactory simulations and high uncertainty in the measurements.

TABLE OF CONTENTS

1 INTRODUCTION

The wind energy sector is currently experiencing a period of unprecedented growth. It is expanding worldwide, powering more of the world with renewable energy. The reason behind this growth is two-fold. Over the last years, wind energy has matured and increased its competitiveness against other energy resources. The main driver, however, is the need for emission free energy. First and foremost to tackle the problems of climate change by reducing the greenhouse gas emissions, but also to phase out air polluting energy resources (WWEA 2014).

This is why the European Union has set a range of goals for how its energy demand is to be generated in the future. By 2020, one fifth of Europe's energy demand is scheduled to come from renewable energy resources (European Parliament 2009), planned to increase to about one forth by 2030 (European Commission 2014). Wind power is playing a big part in this, seeing that 12.8 GW of wind power capacity was installed across Europe in 2014 alone (EWEA 2015). On a global scale, the total installed capacity reached 336 GW by the end of June 2013, enough to generate somewhere around 4 % of the world's energy demand (WWEA 2014).

Because of spatial and economic constraints, and because of the limited number of suitable sites, wind turbines are clustered in *wind farms*. It is advantageous in many ways, but there is one big negative aspect. Wind turbines positioned in close proximity of each other experience the phenomenon of wake effects. A turbine operating downwind of another turbine will stand in the wake of the first turbine, encountering reduced wind speeds, higher turbulence and will most likely generate less energy. According to Barthelmie et al. (2008), wake losses can account for a 10 to 20 % energy loss in large wind farms. In smaller farms, it is often possible to arrange the layout so that the turbines seldom operate downwind of each other. The exact value of the energy loss depends on many factors, for example the local wind regime, terrain characteristics and turbine specifications (Politis et al. 2012).

In order to keep wake losses at a minimum, wind farm designers rely on *wake models* to optimize the turbine layout. Several different types of wake models exist, each with their own pros and cons, and with a varying degree of complexity. Even today, computational limits determine which models are applicable due to calculation time

consumption. Therefore, *kinematic* wake models are often preferred. To ensure that these models function satisfactorily, there is need for validation.

Validating the models requires real data, gathered either in a wind tunnel or in a wind farm. The benefit of using measurements from a wind farm is the fact that the models are tested against non-controlled real-world conditions. The downside of using such data is amongst others the uncertainty (Politis et al. 2012). Recently there has been many wake model studies on offshore wind farms, but not that many onshore. The main reason is that wake losses in general are bigger offshore due to less turbulence intensity over open water, and thereby a reduced recovery of the wake (Hansen et al. 2012). Nonetheless, wake losses in onshore farms can be substantial.

Validating wake models is drastically complicated in complex terrain, which has a big impact on the local wind climate, influencing both wind speed and wind direction (Politis et al. 2012). This has always been a troublesome area for the wind industry. The linearized models have proven to fail in such terrain, so the advance of CFD models offers new hope for better simulations (Landberg 2012).

Both Crespo et al. (1999) and Duckworth and Barthelmie (2008) state that not enough work has been carried out about how wakes and complex terrain interact. The problem is that the solutions differ from site to site. In other words, the solution will always be site-dependent. Nevertheless, identifying trends and tendencies is possible (Politis et al. 2012). And by doing research at more sites it is possible to identify the trends with increasing levels of confidence (Duckworth & Barthelmie 2008).

The main objective of this thesis is to validate three kinematic wake models (the Jensen-, Larsen- and Ishihara model) in complex terrain with the use of computational fluid dynamics (CFD), by investigating how accurate the wake models predict the measured wake, with regard to the normalized power deficit, the wake width and the energy loss. The wake models prediction of the annual energy production (AEP) for each turbine are investigated, and finally a look at the actuator disc approach and its accuracy regarding the wind deficit in the wake. The research is performed under the hypothesis that there are negligible differences in the prediction capabilities of the three kinematic wake models.

2   LITERATURE REVIEW

This chapter will present a brief description of the wake behind a wind turbine and its characteristics. Then, the different wake models and their development will be described, and finally, a look at former research studies within the topic of wake model validation.

2.1   THE WAKE BEHIND A WIND TURBINE

Upwind an operating wind turbine, the speed of the moving air decreases as the turbine acts as an obstacle. At the same time the pressure of the incoming air rises. Crossing the rotor, the air will experience a sudden pressure drop as the turbine extracts energy from the moving air (Crespo et al. 1999).

Downstream, the cylindrical column of air that passed through the swept area of the turbine, expands as the air returns to ambient pressure (Lissaman 1994). This is the *wake* of the turbine, a flow field characterized by reduced wind speed and increased turbulence (Magnusson & Smedman 1999). The size, shape and development of the wake depends on a wide variety of factors (Rados et al. 2009).

The wake is commonly divided into two parts, namely the near- and the far wake (Vermeer et al. 2003), although some authors operate with an intermediate region in between (for example Moskalenko et al. (2010)). The near wake is the part between the turbine and the point where the wake flow is fully developed (Tong et al. 2012). This segment of the wake is highly influenced by turbine characteristics, such as the geometry of the blades (Magnusson & Smedman 1999).

The near wake reaches roughly two to five rotor diameters downstream the turbine. Given that the distances between the turbines in a wind farm (in the prevailing wind direction(s)) usually are greater than this, the near wake itself is not that important concerning wind farm wake modeling. But it cannot be ignored, as the far wake depends on it (Vermeer et al. 2003).

Due to the difference in wind speed between the wake and the ambient free stream, a shear layer forms around the wake. This layer expands downwind, until the point where the shear layer reaches the wake center and the wake is said to be fully developed (Sanderse 2009).

Now, the wake enters the far wake region, where the velocity deficit may be assumed having an axisymmetric and self-similar profile. But, the presence of both the

ground and the shear of the ambient flow partially invalidates this assumption (Frandsen et al. 1996). Nonetheless, the analytical wake models are based on this. In the far wake, the only characteristics that stem from the turbine is the thrust coefficient and the turbulence generated by the rotor (Crespo et al. 1999).

An important property of the wind is turbulence. It is defined as "deviations of the instantaneous wind speed from the mean wind speed over an interval of time" (Rohatgi & Barbezier 1999). The atmospheric turbulence level depends on the surface roughness, the stability of atmosphere and the height above the ground. Mechanical turbulence on the other hand originates from the turbine itself. It is caused by the turbines blades, nacelle and tower, and decays fast (Sanderse 2009).

The mixing effect of turbulence is of high importance in regard to the wake development. Fast moving air from outside the wake is drawn into the wake, helping the slow moving air inside the wake to regain speed (Sanderse 2009). So the more turbulence, or in better words, a higher turbulence intensity, the faster the air inside the wake returns to ambient speed, implying a reduced wake distance.

The stability of the atmosphere is known to have a big impact on the wake and its recovery (Landberg 2012). It is caused by the temperature gradient in the atmosphere. On a sunny day, the ground heats up and warms the air at low altitudes. This causes the temperature to decrease with height and the atmosphere is unstable. A high mixing of the air occurs. At nighttime or in the winter, the temperature gradient reverses. The temperatures increases with height and the atmosphere is stable. Very little mixing of the air occurs, resulting in a high wind shear. The intermediate state, when the temperature is constant with height, is called the neutral state and is characterized by little mixing. The stability of the atmosphere usually follows a daily cycle, but on cloudy days a constant neutral condition is often observed (Rohatgi & Barbezier 1999).

The thrust coefficient of the turbine generating the wake determines some of the wake properties. The power deficit of a turbine in the wake is high when the turbine in front operates at a high thrust coefficient (Elliott 1991). The wake width also depends on the thrust coefficient (Sanderse 2009).
So, any turbine positioned in the wake of another turbine will experience a reduced energy output. Due to the increased turbulence, a turbine in the wake will also experience increased loading and possibly a higher risk of fatigue (Thomsen & Sørensen 1999).

2.2 WAKE MODELS

Research on wake models started in the late 1970's (Schlez & Neubert 2009). Wake models are used to determine the wind velocity deficit downwind of an operating wind turbine (Duckworth & Barthelmie 2008). Early and innovative work on the subject was published by Lissaman, describing the wake in detail and presenting the first kinematic wake model (Lissaman 1979). A few years later, Jensen described a very simplified kinematic wake model (Jensen 1983). The old work reflects the computational limitations at the time. Yet they have proven to work reasonably well, which is why they are still in use.

Of interest in the context of this thesis is the kinematic wake models, one of the two branches of analytical wake models. The other branch is field models, which calculate the entire flow field around the wake and naturally require considerably more computational power and time (Duckworth & Barthelmie 2008). The Ainslie model is an example of such a model (Ainslie 1988).

The kinematic wake models, in contrast, are fast to use. They are based on conservation of momentum and an assumption of self-similarity. The velocity deficit is assumed uniform in the cross-section of the wake, so the thrust of the turbine can be used to calculate the velocity deficit. The kinematic wake models are known to produce acceptable results (Crespo et al. 1999).

2.3 FORMER VALIDATION STUDIES

There are many validation studies of wake models, especially on the frequently used analytical wake models. However, there are few validation studies in complex terrain, which might stem from the fact that there are many difficulties related to these kinds of studies (Crespo et al. 1999).

Politis et al. (2012) performed a study on wake effects in complex terrain. It emphasizes the difficulties of accurate modeling in complex terrain, stating that "the modeling of wake effects in complex terrain becomes ambiguous since there is no obvious reference wind speed". In this study, CFD methods were used to both calculate the wind farm AEP and to look at the wake flow. The authors highlight the challenges regarding wake modeling in complex terrain.

Duckworth and Barthelmie (2008) described methods used for validating wake models, focusing on two kinematic wake models (the Katic- and Larsen model) and the

field model by Ainslie. Data from two onshore farms in the UK were used. The study compared measurements and the wake models predictions of the normalized power in the wake and of the wake width. The Ainslie model performed best. Then followed the Katic model and finally the Larsen model.

In the master's thesis by Renkema (2007), the wake models included in WindPRO are validated. This includes the Jensen model, the Larsen model and the Ainslie model. The study used measurements from two onshore wind farms and from a wind tunnel, and found large differences in accuracy of the models. The Larsen model performed badly, while the Jensen-model (with modification) performed reasonably well. The Ainslie model was clearly the most accurate.

3 MATERIALS AND METHODS

This chapter presents the data used in this thesis and the methods used to answer the research question. The research area is presented in chapter 3.1. Chapter 3.2 introduces the data sets and explains the filtering process. The WindSim software and the simulation process is shown in chapter 3.3, and the kinematic wake models are described in chapter 3.4. Finally, chapter 3.5 outlines the validation procedure.

3.1 NYGÅRDSFJELLET WIND FARM

Nygårdsfjellet wind farm (68°30' N 17°52' E) is located in the northern part of Norway, twenty kilometers northeast of Narvik. The wind farm consists of 14 wind turbines, situated around 400 meters above sea level and within an area of roughly 1.5 square kilometers. The first phase of the wind farm was established in 2006, consisting of three Siemens SWT 2.3 MW 93 turbines. The second phase in 2011 saw the addition of 11
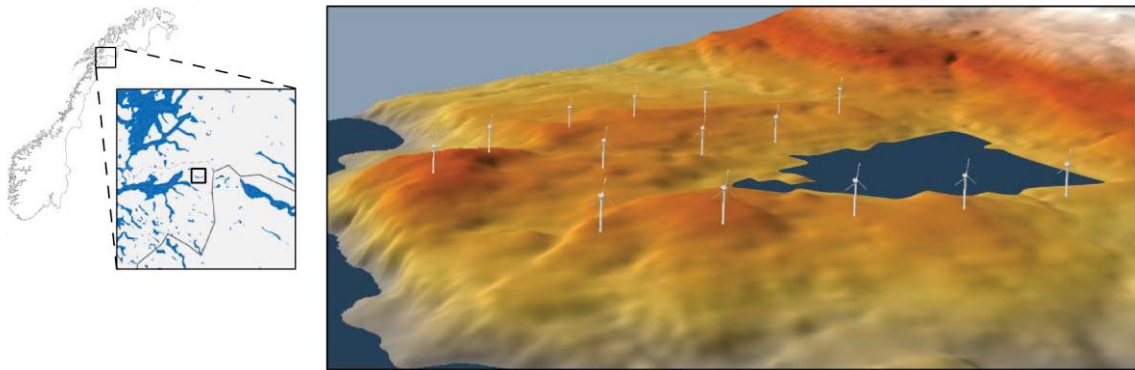

Figure 1. Map of Nygårdsfjellet wind farm, with a computer-generated 3D-view of the farm layout looked upon from the southeast with the turbines facing east.

Siemens SWT 2.3 MW 93 turbines, adding the installed capacity up a total of 32.2 MW. All the turbines have a hub height of 80 meters. They are positioned in the north-south direction, in what best can be described as three non-parallel rows as can be seen in Figure 1 above. The distance between the turbines in the prevailing wind direction varies from roughly 4.5 to 10 D, while the "in-row" distance is somewhere above 3 D. The wind farm is located in complex terrain, with a range of hills and steep slopes. Lake Jernvannet partially surrounds the farm in the south, and there is also a lake located inside the farm.

Wind measurements performed at the site shows strong steady winds with a mean of 8.5 m/s at 80 m above ground level. The prevailing wind direction at the site is from the east, as the wind rose from the met mast shows in Figure 2, but there is also some winds from the west. A seasonal pattern exists, with winds from the east more frequent in the winter, and vice versa. Also, wind speeds are higher during the winter than in summer, and there are few periods of extreme winds (Nordkraft). Due to the climate at the site, icing of the turbine blades sometimes causes energy losses (Homola et al. 2009).
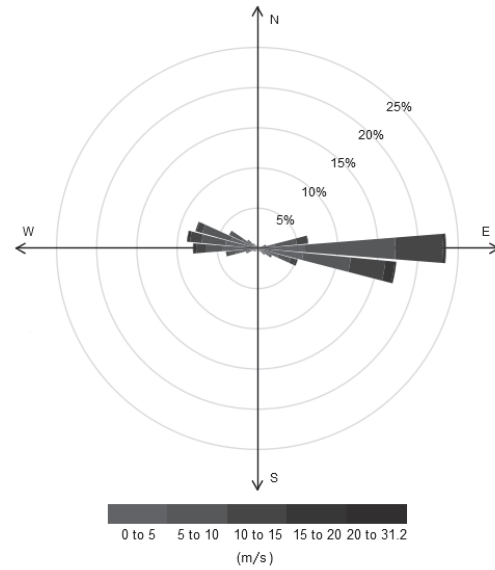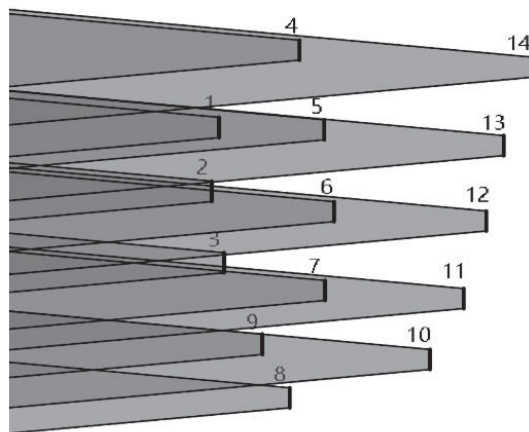

Figure 2. Wind rose with ten-degree bins from the met mast for the entire year.

3.1.1 Wake Cases

In order to validate the wake models there is a need for some wake cases. Pinpointing the most interesting cases is done by comparing the wind farm layout with the wind rose from the met mast. Seeing that there are two dominant wind directions, two figures are made to easily identify the wake cases, one with wind blowing directly from the east and another with wind directly from the west. For illustrative purposes, the wake is assumed to expand linearly and that the wind direction is the same over the entire wind farm (neglecting terrain effects and natural fluctuations). Turbines are numbered from 1 to 14, where turbine 1, 2 and 3 are the turbines from the first

Figure 3. Wake formation with wind coming directly from the east.

phase. In the first plot (Figure 3, with wind from the east) turbine 4, 5, 6, 7 and 9 are in the wake of turbine 14, 13, 12, 11 and 10 respectively. Turbine 8 is in the wake of turbine 10 when the wind comes from the northeast. Turbine 1, 2 and 3 are totally or partially in a double wake. In the second plot (Figure 4, with wind from the west) turbine 14, 5, 6 and 10

are in the wake of turbine 4, 1, 2 and 9 respectively. Turbine 7 is in the wake of turbine 3 when the wind comes from the northwest. Turbine 13, 12 and 11 are totally or partially in a double wake. Eleven single-wake cases (and six double-wake cases) are now identified. Since this thesis will focus on single-wake cases, the double-wake cases are dropped. And, due to few data points in the wake cases '13-5' (turbine 5 in the wake of turbine 13), '14-4' and '9-10', these are not further investigated. The eight remaining single-wake cases are summarized in Figure 5 below.
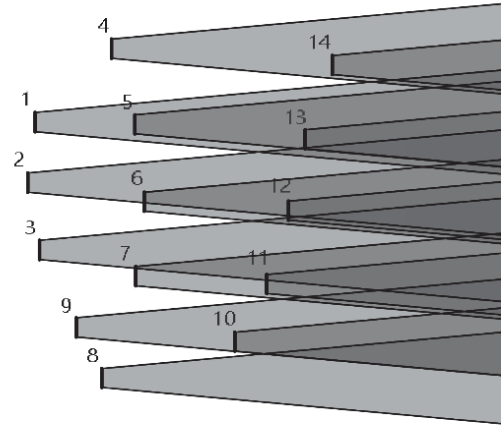

Figure 4. Wake formation with wind coming directly from the west.
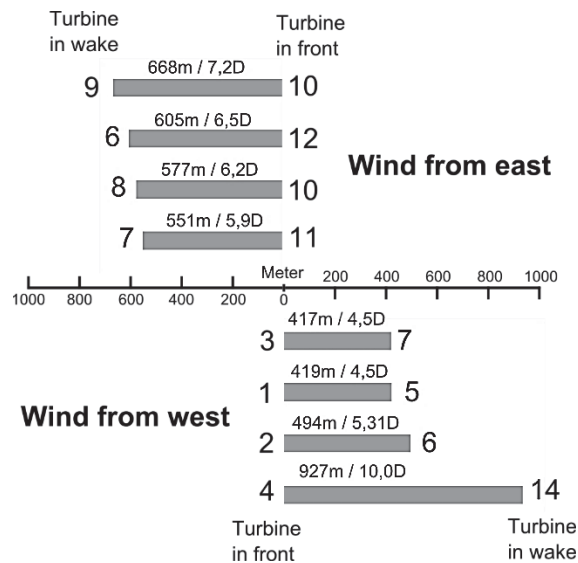

Figure 5. The eight single-wake cases investigated in this thesis, with the distance between the interacting turbines given in meters and in rotor-diameters.

The entire wind farm layout, with the turbine in-between distance and the centerline angle, is shown in Figure 6 below.
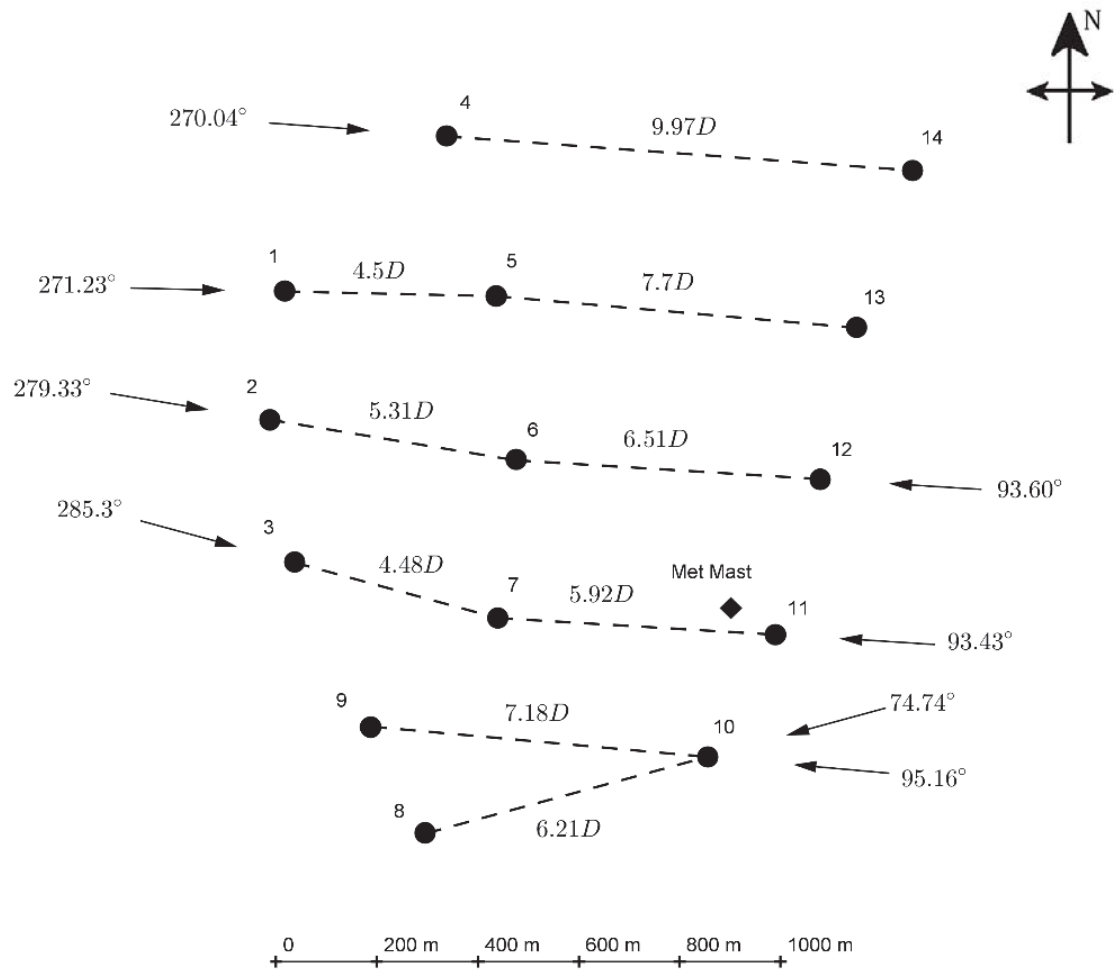

Figure 6. The turbine layout at Nygårdsfjellet wind farm. The in-between distance of the turbines are marked, and also the centerline angle for the eight wake cases under investigation.

3.2 DATA AND DATA FILTERING

The data from Nygårdsfjellet wind farm covers an entire year, ranging from 1/1 until 31/12 2013. This includes production data from the fourteen turbines and the meteorological mast, each containing 10 minute-average data. All the datasets contain some periods with no recordings, possibly due to errors with the loggi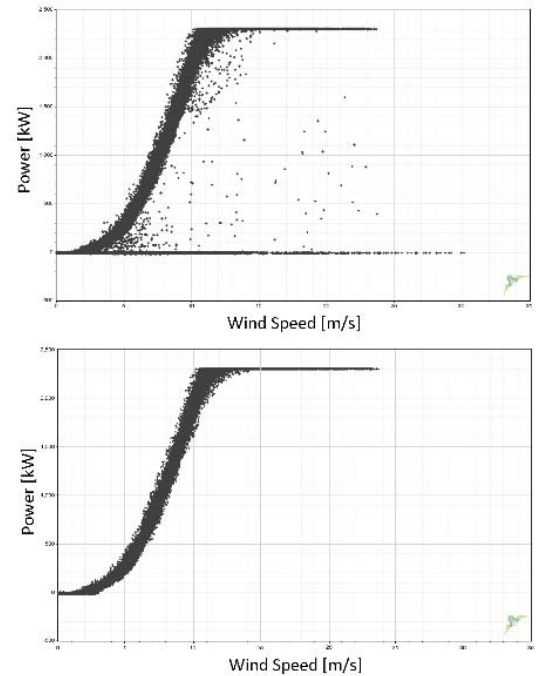ng system (M. Homola 2015, pers. comm.). The data from the turbines includes power production, yaw angle, wind speed from the two anemometers positioned at the hub and blade pitch. Recordings from the meteorological mast includes wind speed at three different heights: 40, 30 and 20 meters. The maximum and minimum wind speed recorded in the 10 minute-time step is recorded, including the standard deviation. The wind direction is recorded at two heights: 40 and 20 meters. The mast also records temperature.

Figure 7. Result of the data filtering process for one of the turbines. Unfiltered at top, filtered below.

The data filtering was performed in the Windographer software. Removal of invalid data points is necessary to produce credible results not influenced by recording errors and icy conditions. Each turbine went through the following filtering criteria:

- Power < 0 (removes all data points where the turbine is at standstill)
- Manual removal of data points that deviate largely from the power curve.

Figure 7 illustrates the result of the filtering process for one of the fourteen turbines. Due to a problem with the anemometers at both 20 and 30 meters at the meteorological mast, only the data recorded at 40 meters was used. This data was filtered by removing data points where the anemometer recorded 0.4 m/s (NULL-value) for four consecutive recordings.

3.3 SIMULATIONS

Simulations are performed in the commercial WindSim software. The software is based on computational fluid dynamics (CFD) technology, solving Reynolds Averaged Navier-Stokes equations (Crasto et al. 2012). The CFD simulation is steady-state, which means that for a given boundary wind direction, the model assigns a converged wind direction for all cells in the simulation (Berge et al. 2006). The fluctuating nature of the wind is therefore not taken into account (Politis et al. 2012). The CFD model also assume a neutral stratification of the atmosphere. In the CFD simulations, the speed-up due to the terrain and the wind speed deficit due to wakes are simulated in two separate processes (WindSim 2009). WindSim is a module-based software. First, the terrain and roughness data is used as input. The original file contains data from a 40 by 40 km area with a 20 meter grid resolution, but this is cropped into a 10 by 10 km area in order to reduce the number of cells. A refinement is placed over the wind farm, which is positioned at the center of the grid. The terrain data is also smoothened in order to reduce the risk of divergence in the wind field-simulation. The total number of cells in the final simulation is 1.3 million, with 30 vertical layers (Figure 9). Figure 8 visualizes the terrain discretization and refinement.
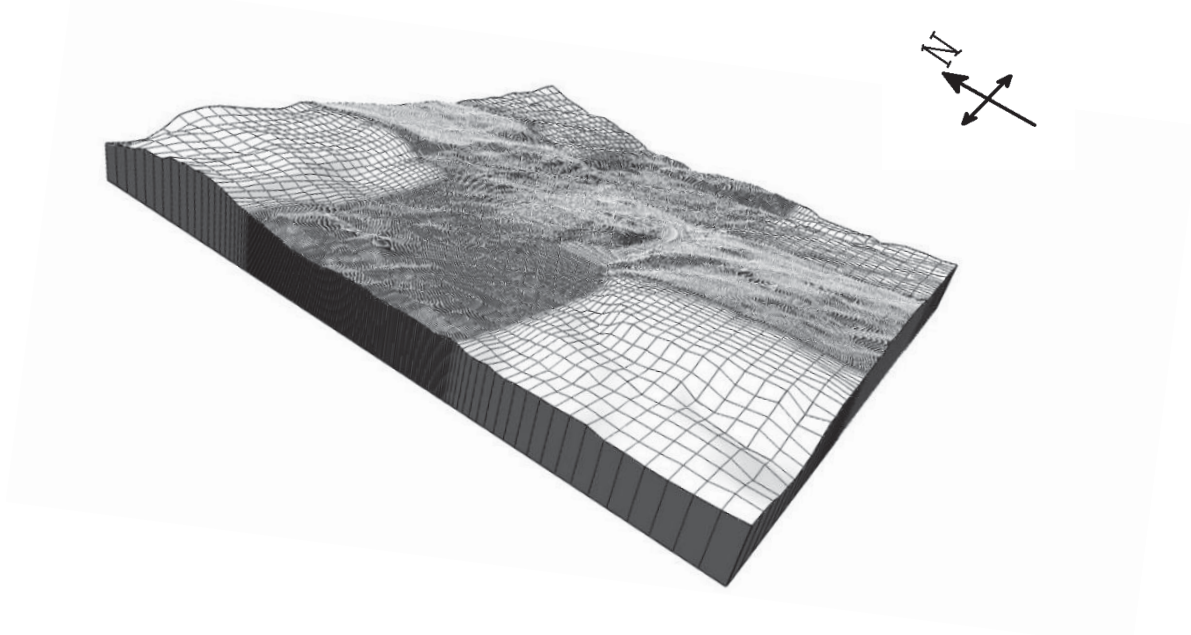

Figure 8. The terrain discretization used in the final simulation (trial 5). The refined area located over the wind farm the in center.

WindSim then calculates the entire wind field over the area, estimating the speed-up due to the terrain, for a given number of wind directions. In this case, 36 directions are used, i.e. a 10° separation. Then, the wind measurements from the met mast is added (referred to as the 'climatology-file'), with both speed and wind direction recorded at 40 meters at the met mast. The wind farm layout and the turbine power curve are added. All the parameters used in the final simulation (trial 5) is shown in Table 2.

Table 1. Model parameters in the final simulation (trial 5)

| Model area	10x10 km
Number of cells	1.3 million
Height of model	6432 m
Number of vertical layers	30
Refinement area	3.3 x 3.3 km
Cell size in refinement area	20.3 x 20.3 m
Air density	1.225 kg/m^3
Wind field sectors	36
Turbulence model	Standard k-ε
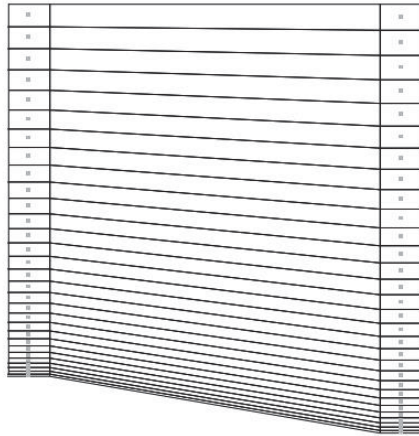
Figure 9. The vertical layers in the simulation, distributed with more cells close to the ground.

In the 'Energy'-module, WindSim provides several export options. One of them contains the power production of each turbine in every time step provided in the climatology-file. The software uses the power curve to convert the calculated wind speed into the turbine power output. Selecting which of the three wake models to employ is done in this module. Exports of the wake velocity deficit predicted by each wake model (simulated in the "Wind Resources"-module) are shown in   Appendix A.

3.3.1 Grid Independence

The result of the simulations have been tested for grid independence. This means that a further refinement of the grid will yield no change in the solution (De Souza 2005). First, the speed-up at the turbine locations was tested. At the 1.3 million cell-trial (trial 5), the change from the 1.1 million cell-simulation (trial 4) is very small for all turbine locations (as can be seen in Figure 10). This indicates that some sort of convergence has taken place and it is assumed that the solution is grid independent.
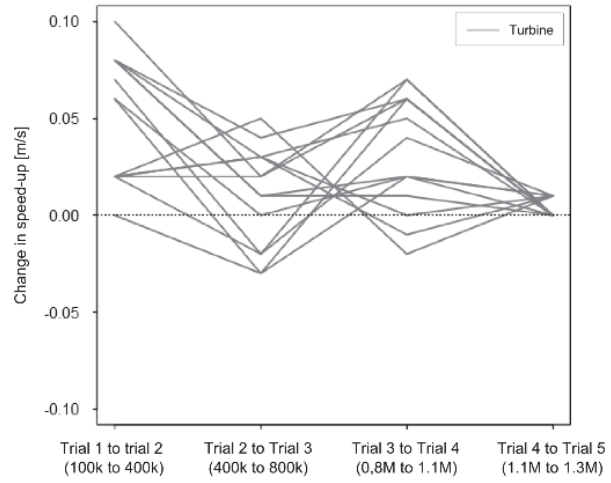
Figure 10. Change in speed-up at turbine locations between the performed simulations. Number of cells in each trial is given.
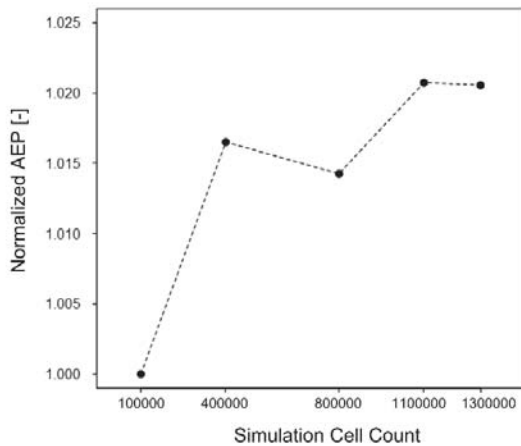

Figure 11. Normalized AEP (normalized to the first simulation) against increasing number of cells.

In addition, Figure 11 shows that the farms AEP (normalized to the first simulation) also converges at 1.3 million cells (trial 5). This increases the confidence in the achievement of a grid independent solution.

3.3.2 Actuator Disc

Another feature in the WindSim software is the actuator disc. The turbine rotor is modeled as a momentum-extracting disc by using porous cells. These cells exert a resistive force on the wind, based on the thrust coefficient of the turbine, which is distributed over the turbines swept area. The result is a wind velocity deficit and an increased turbulence intensity downstream the turbine (Crasto et al. 2012). This implies that the interaction of the terrain and the wake is simulated simultaneously, and not separately as in the original simulations (Chapter 3.3). The WindSim software recommends the use of at least 16 cells over the turbine diameter, in this case cells of roughly 5 meters. Due to computational limits, only 12 cells were used in the simulations.

The actuator disc approach is employed on the single-wake case '1-5', with turbine 5 in the wake of turbine 1, for a wind direction of 270°. Simulations are preformed for various wind speeds above the boundary layer. To check how well the simulation match the measurements, the simulated speed is found at the rotor center for both turbines. A look up in the measurements is then performed, finding the wind speed at turbine 5 when the wind speed at turbine 1 is ± 0.5 m/s off the simulated value and the yaw is within the range of 270 ± 1°. The standard deviation of the measurements is calculated.
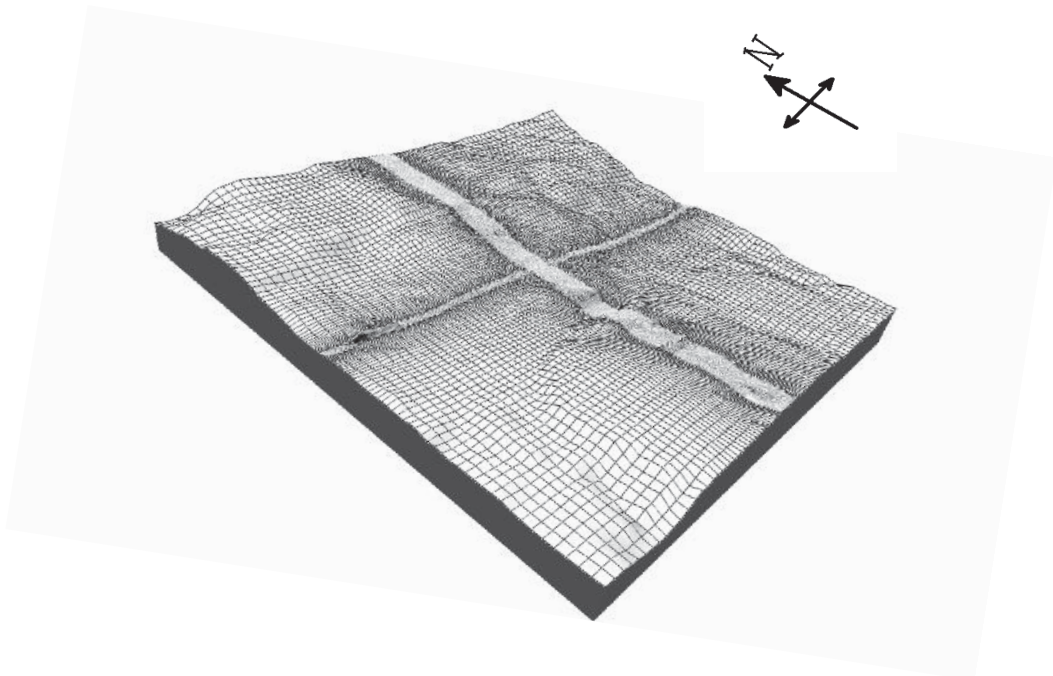
Figure 12. The terrain discretization used for the actuator-disc simulation.

3.4 KINEMATIC WAKE MODELS

There are three kinematic wake models available in the WindSim software. This includes the Jensen model, the Larsen model and the Ishihara model. In the form written, the models calculate the normalized velocity deficit: $\delta V = (U-V)/U$, where U is the free stream velocity and V is the wake velocity.

Jensen model

Assuming a linear expansion of the wake, the kinematic model developed by N. O. Jensen (Jensen 1983) is one of the simplest wake models. It was published in 1983, but later refined by Katic et al. (1987), and is therefore in some literature referred to as the Katic model. In this paper, it is referred to as the Jensen model. An important parameter is the wake decay constant k, which describes the expansion of the wake and by that also the decay of the wake. The normalized velocity deficit is given by the equation:

Equation 1

$$\delta V = \frac{1 - \sqrt{1 - C_T}}{\left(1 + \dfrac{2kx}{D}\right)^2}$$

Where C_T is the thrust coefficient, x is the downwind distance, k is the wake decay factor and D is the rotor diameter. Due to this formulation, the model assumes a "top-hat" wake profile, i.e. a constant velocity deficit throughout the cross-section of the wake.

Larsen model

Based on the Prandtl turbulent boundary layer equations, the Larsen model (Larsen 1988) is more complex than the Jensen model. It assumes incompressible and stationary flow and it neglects the wind shear. The normalized velocity deficit is given by the equation:

Equation 2

$$\delta V = \frac{\left(C_T A x^{-2}\right)^{\frac{1}{3}}}{9} \left\{ r^{\frac{3}{2}} \left(3 c_1 C_T A x\right)^{-\frac{1}{2}} - \left(\frac{35}{2\pi}\right)^{\frac{3}{10}} \left(3 c_1^2\right)^{-\frac{1}{5}} \right\}^2$$

Where C_T is the thrust coefficient, A is the swept area of the turbine, x is the downwind distance, c_1 is the Prandtl mixing length and r is the radial distance. Due to the models

dependency of the radial distance, the velocity deficit varies in the cross-section of the wake, contrary to the Jensen model.

Ishihara model

In 2004, Ishihara et al. developed a new kinematic wake model (in this thesis referred to as the Ishihara model) that takes the effect of turbulence on wake recovery into account (Ishihara et al. 2004). This is different from the two former models that predict a constant wake recovery. The normalized velocity deficit is given by the formula:

Equation 3

$$\delta V = \frac{C_T^{\frac{1}{2}}}{32} \left(\frac{1.666}{k_1} \right)^2 \left(\frac{x}{D} \right)^{-p} \exp\left(-\frac{r^2}{b^2} \right)$$

Where C_T is the thrust coefficient, k_1 is a constant, x is the downwind distance, D is the rotor diameter, r is the radial distance and b is the part that incorporates the turbulence, both the ambient and mechanical.

Wake model settings

WindSim provides options for some wake model parameters and how the wake is modeled. The wake decay constant in the Jensen model is calculated from the roughness height at the site. The default setting in WindSim is to read this value from the roughness data, and this is also the choice for the simulations run in this thesis. For both the Larsen- and Ishihara model, the turbulence intensity is read from the generated wind database, which is the default option in WindSim. The influence range of the wake is another option, i.e. how close to and how far from the turbine the wake is calculated. Simulation are run with the range: 1 to 50 D. The choice on how multiple wakes are treated is also present. In these simulations, the wake deficits are added as described by Equation 4 below.

Equation 4

$$\delta u = \sqrt{\delta u_1^2 + \delta u_2^2 + ... + \delta u_n^2}$$

3.5 VALIDATION PROCEDURE

To validate the three kinematic wake models, a procedure is defined in order to investigate how the models fit the measured data. A part of it is in line with the validation procedure employed by Duckworth and Barthelmie (2008). The procedure runs as follows:

- Profile of the normalized power deficit in the wake
- Power deficit at the wake centerline
- Wake width
- Energy loss in the wake
- Normalized turbine AEP

Each of these points will be described in detail in chapter 3.5.3. But first, due to the complex terrain, there are some issues that complicates the validation process and needs to be resolved.

3.5.1 Issues Complicating the Validation Process

First, the peak of the wake, both measured and modeled, is not directly at the centerline between the turbines. This might indicates that the wake is influenced by topographic effects (Duckworth & Barthelmie 2008). The problem is that the modeled wake is not overlapping the measured wake. Politis et al. (2012) mention four possible explanations for this observed shift, where two of them are associated with the measured data and two with the modeled data: yaw misalignment of the turbines, uncertainty of the measured data, grid independence is not achieved and inaccurate calculation of the reference wind speed. Since this observed shift is an issue not related to the wake models, it is solved by shifting the measured wake so that the wake peak/centerline of both the measured and modeled data overlap. Duckworth & Barthelmie also employed this method. The method is shown in Figure 13.
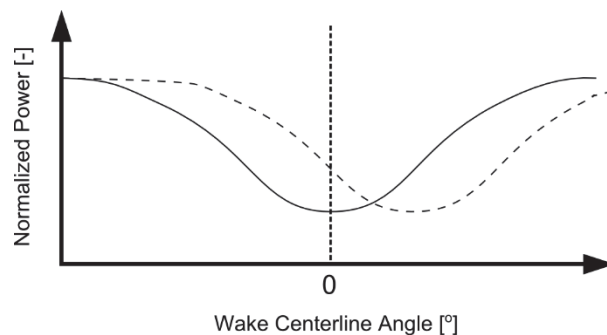
Figure 13. Correction method for the observed wake shift. The measured wake is shifted so the peak of the wake is directly at the wake centerline.

18

Another challenge is that the turbines, due to topographic effects, operate under different conditions. The speed-up caused by the terrain will depend on both the position of the turbine and on the wind direction. The result is that the turbines will most likely not have the same power output for a given wind speed (assuming both are in a free-stream (i.e. no-wake) situation). In the investigation of a wake case, this causes some problems, as the normalized power in the no-wake region will deviate from unity and will also possibly be different at the two sided of the wake. The estimation of the wake width is therefore made more difficult.

Figure 14 plots the measurements of the frequency of the yaw angle for westerly wind for seven of the turbines including the met mast. Although there are some variance in the yaw direction, which may be attributed to terrain effects, the measurements from turbine six stands out. Something is clearly not right with the measurements. If that wasn't the case, the turbine would operate with a very high degree of yaw misalignment (if the possible contribution of the terrain is ignored). This seems unlikely. Calculations indicates that the recordings are off by roughly twenty degrees.
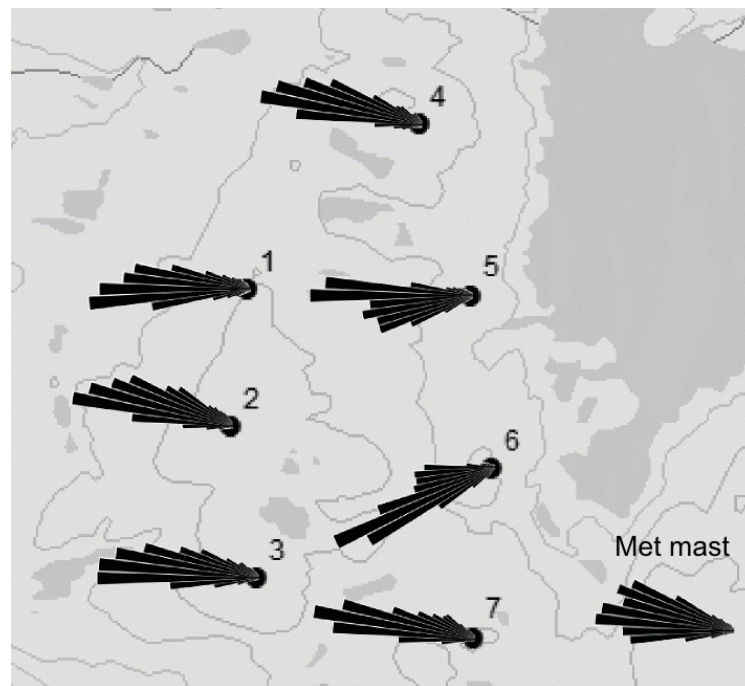
Figure 14. Measurements of the wind direction frequency from the west at seven turbines including the met mast. The wind roses are composed of five-degree bins.

Another visible feature in the figure is the more widely spread recordings at the met mast compared to measurements from the turbines which shows a more narrow range of wind

directions. Also the simulation indicates that there is some error in the directional recordings at turbine 6, as seen in Figure 15. The frequency of the modeled wind direction is shown to come from a west- northwesterly direction, quite similar to the measurements at the met mast and certainly more realistic than the measurements.
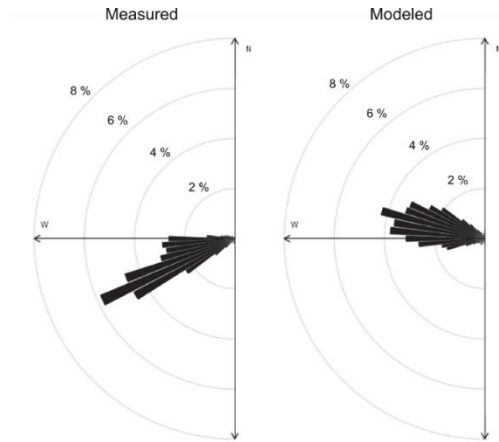
Figure 15. Comparison of the measured and modeled wind direction frequency for westerly winds at turbine 6 with five-degree bins.

From this comparison, it is also evident that the higher spread of the wind directions at the met mast influences the modeled data.
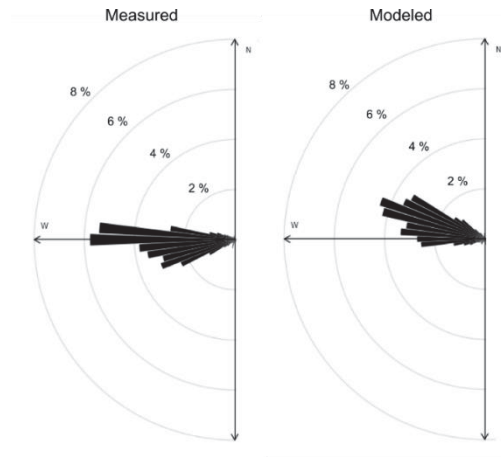
Figure 16. Comparison of the measured and modeled wind direction frequency for westerly winds at turbine 5 with five-degree bins.

At turbine 5, the simulated westerly wind directions also deviates from the measurements (Figure 16). From the measured data, the turbine is seen to receive winds directly from the west quite frequently. At that wind direction, it stands in the wake of turbine 1. The modeled data, however, predicts the wind to come from a more northwesterly direction,

which happens to be directions where the turbine operates in free-stream winds. Far fewer instances of a direct westerly wind are estimated and thereby fewer instances where turbine 5 operates in the wake.

Finally, the CFD simulation over estimates the speed at turbine location. Figure 17 shows the distribution of the power output of turbine 1. The count of time steps with an output around rated power production are seen to be higher in the simulated data compared to the measurements.
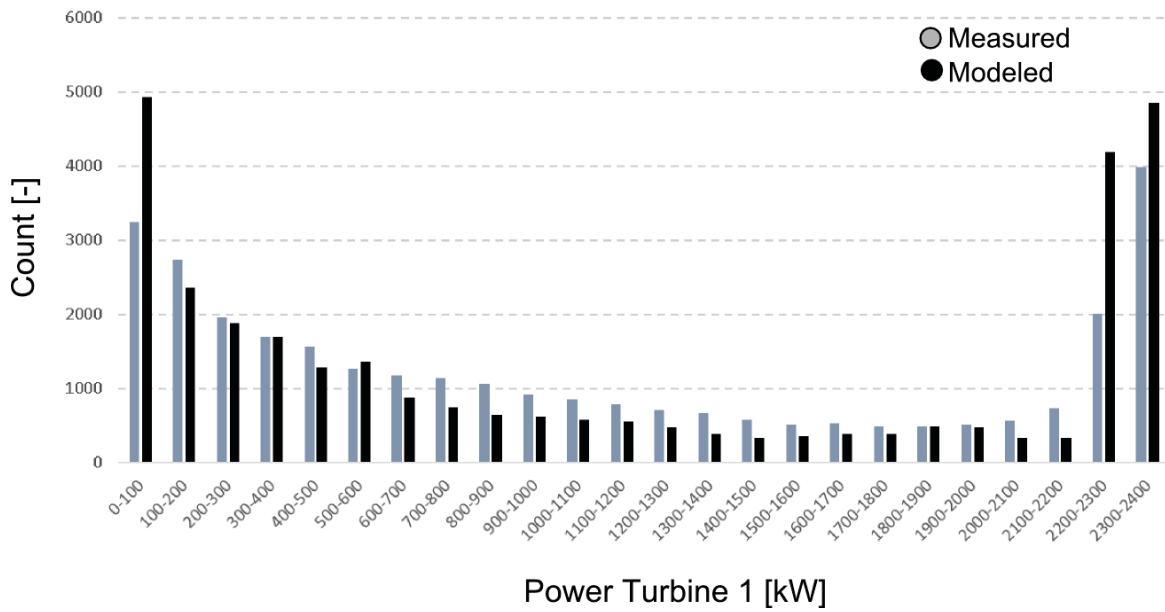

Figure 17. The distribution of the power output of turbine 1, for both measured and modeled data.

3.5.2 Choice of Speed Interval and Yaw

The validation procedure calls for a defined interval of the free stream wind speed. Looking at the thrust curve of the turbines (Figure 18), it is clear that the maximum wake will occur when the turbine in front is experiencing winds around 9 m/s. At this speed the turbines thrust coefficient is at maximum (0.87). To ensure enough data points, the speed interval of 9 ± 1 m/s is chosen. This speed interval is used throughout the thesis, except in the analysis of the
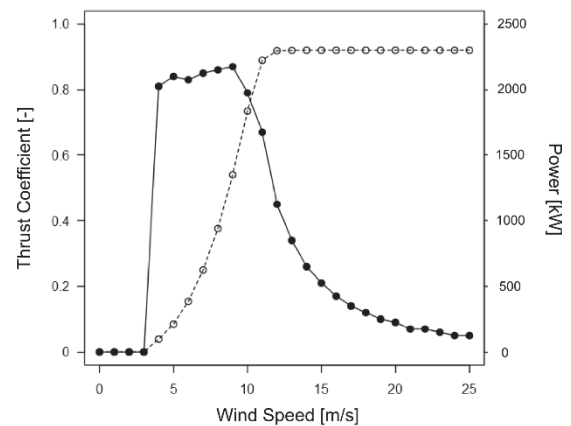

Figure 18. Thrust coefficient and power output of the Siemens SWT 2.3 MW 93 turbine as a function of wind speed.

normalized power at the wake centerline versus wind speed. The manufacturer's power–
and thrust coefficient curve of the Siemens SWT 2.3 MW 93 are used in the modeling of
all turbines without modification. The yaw angle of the turbine *in the wake* is used in the
validation procedure, unless stated otherwise.

3.5.3 Details of the Validation Procedure

Profile of the normalized power in the wake

The profile of the power deficit is examined by using the eight single-wake cases identified
in chapter 3.1.1. The filtered measured data (Ch. 3.2) and the data from the three wake
models (Ch. 3.3) are then used to obtain the normalized power deficit in the wake. For
each time step, the normalized power is calculated as described in Equation 5 below:

Equation 5

$$\text{Normalized power} = \frac{P_{Wake}}{P_{Freestream}}$$

The power of the turbine in the wake is divided by the power of the turbine in front (free-
stream condition). The calculated data are then grouped in bins of 2.5°, based on the yaw
of the turbine in the wake and the mean normalized power is calculated within each bin.
For the measured data, the standard deviation is calculated for each bin.

Normalized power at the wake centerline

The next phase of the validation procedure is to quantify the results obtained from the
profile of the normalized power in the wake, regarding the wake models prediction of the
centerline, i.e. maximum, power deficit. The mean absolute error is calculated, given as the
absolute difference between the mean of the measured data and the model prediction at the
centerline of the wake ± 1°. The results are presented in boxplots.

An aspect of the wake models representation of the centerline power deficit is lost
when examining the absolute error – Are the models over- or underestimating the
centerline power deficit? – To answer this, the mean error is calculated.

Since the previous phase of the validation procedure only examined a narrow interval of the free stream wind (9 ± 1 m/s), it is important to test how the wake models predict the centerline power deficit for other speeds. The calculated normalized power at the wake centerline of both the measured and of the three wake models are plotted against the free stream wind speed. Wind speed bins of 1 m/s are employed (X ± 0.5 m/s).

Wake width

The wake width is an important property of the wake and is here identified by using Barthelmie et al.'s definition, where the wake width is defined as the: "Distance on each side of the centerline at which the power deficit is within ± 5 % of the free stream power" (Barthelmie et al. 2010).
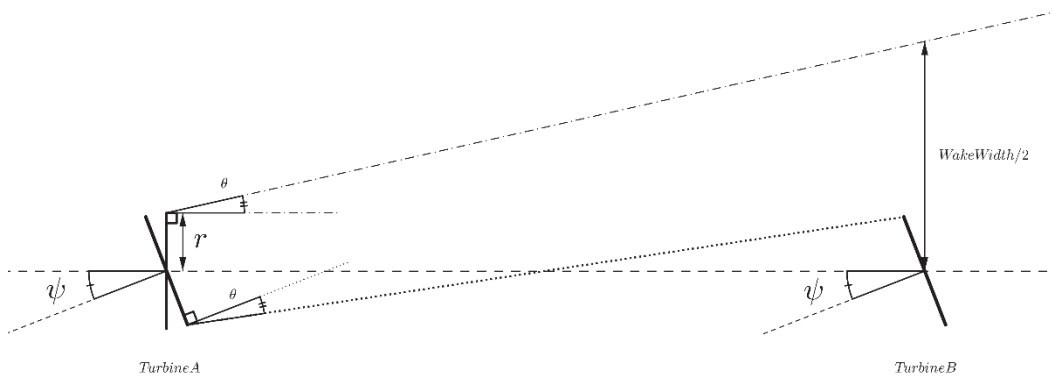
Figure 19. A schematic illustration of the wake width. The angle ψ is the yaw angle of turbine B (in the wake) where the turbine no longer operates in the wake of turbine A. The wake expansion angle, θ, is then a function of ψ and the distance between the turbines. The wake width can then be calculated.

The wake width is found by:

- Using Barthelmie et al.'s definition to find the angle ψ (see Figure 19)
- Using ψ and the distance between the turbines to find θ
- Using θ to find the wake width

The calculated wake width is then normalized to the diameter of the turbine in front.

The wake models accuracy in the estimation of the wake energy loss is of course of high interest. For the simulated data, this loss is easy to obtain, as it is possible to run the simulation where wake losses are neglected and simply subtract the values found in simulations *with* wake losses. What remains is the wake energy loss. For the measurements, however, it is not that simple, since no measurements are obtainable from a wake case where the wake losses are excluded. But, the energy loss in the wake can be found by integrating the power difference between the two turbines with respect to time for all wake situations. Because there are holes in the datasets, the datasets are appended to make sure an equal number of data for both measurements and simulations, i.e. that the total time is equal, and that there is valid data at each time step. Three wake cases are investigated: '1-5', '2-6' and '3-7'.

Seeing that the simulation fails to accurately predict the measured wind direction at the turbine location, as was evident in Figure 15 and Figure 16, a correction procedure is employed in order to see how the models would perform if the simulation were more accurate. So, to correct, the output of each of the three models are used together with the wind direction frequency measured at the turbine, instead of the modeled wind direction frequency.

Turbine AEP

Because of unequal number of measurements and modeled data, it is not possible to directly compare the measured and modeled annual energy production for each turbine. A normalized approach is proposed, making it possible to see if the simulations (and the wake models) capture the trend in the measurements. For the measurements and data from each of the wake models, each turbine's AEP is normalized to the mean AEP of all the turbines. Then it is possible to compare measured and simulated data.

4 RESULTS

The three wake models prediction of the profile of the normalized power in all eight single-wake cases show substantial differences between the models. Figure 20 and Figure 21 show the investigated wake cases, comparing the measured and modeled normalized power in the wake. The wake-cases shown in Figure 20 are the cases that closely resemble the characteristic "U"-shape. In the last four cases, shown in Figure 21 , the wake shapes deviate from the expected shape.
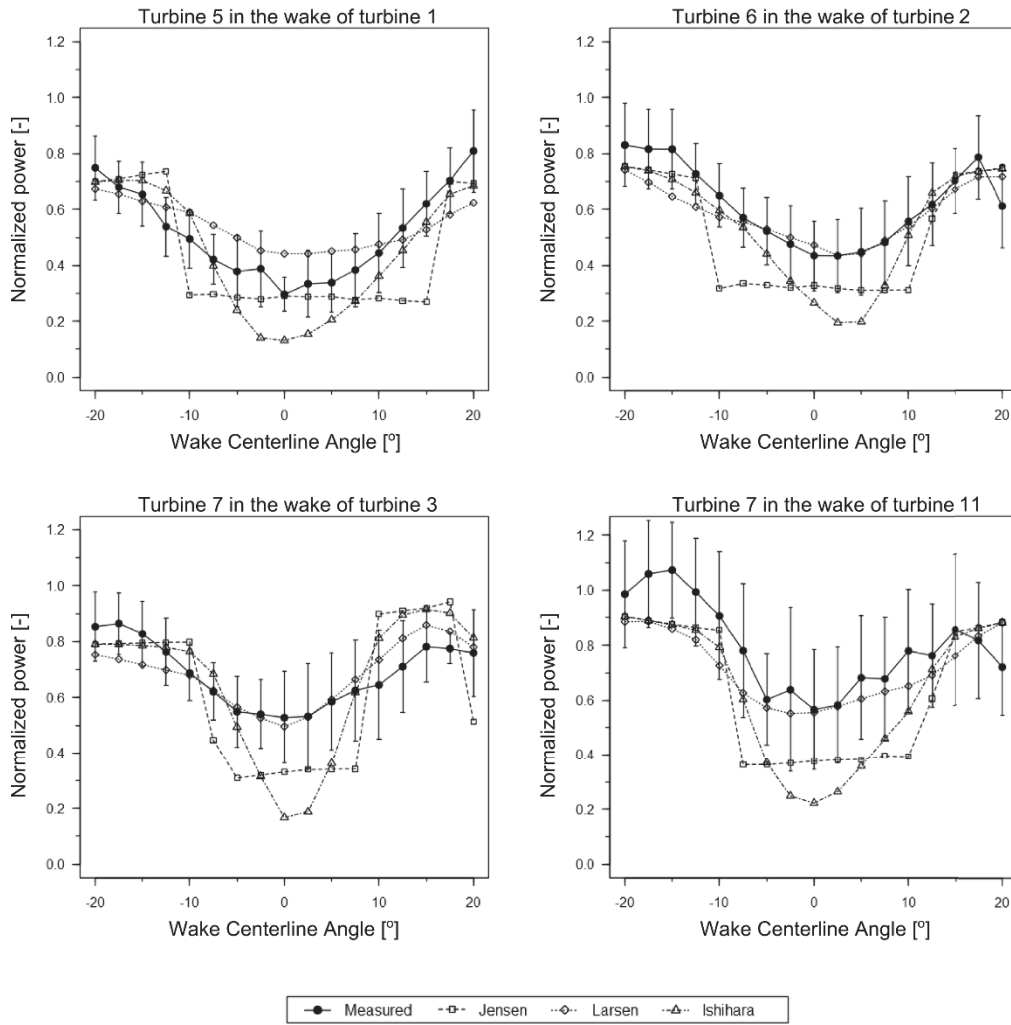

Figure 20. The normalized power for four of the wake cases, ± 20° of the wake centerline, for free-stream wind speeds of 9 ± 1 m/s. The plot shows the measured data and the data from the three wake models. Whiskers represents one standard deviation from the mean of the measured data.

Some trends are clear from the plots in Figure 20. The Ishihara model overestimates the peak power deficit in all cases. The Jensen model with its characteristic top-hat profile also overestimates the peak power deficit, but not to the same extent. Last, the Larsen model correlates well with the measured data in three of the four cases.
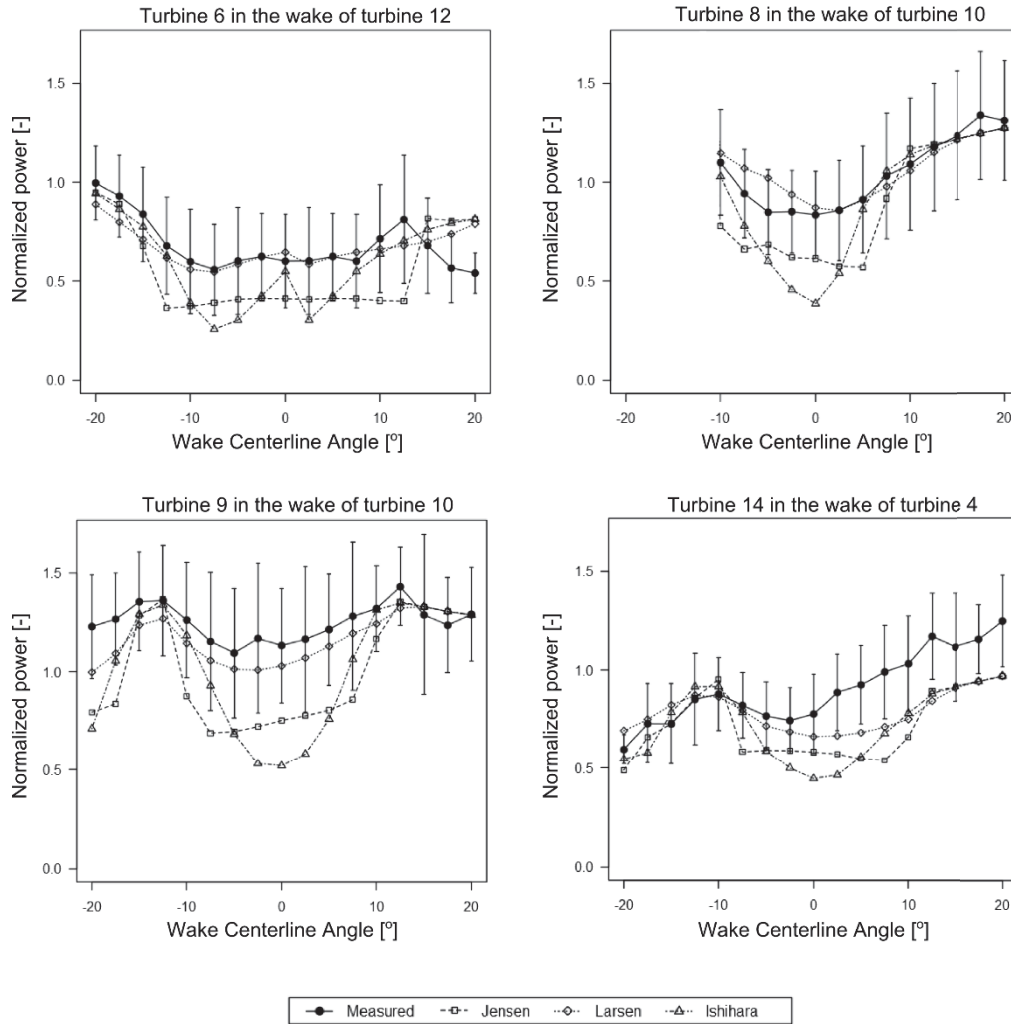

Figure 21. The normalized power for four of the wake cases, $\pm 20°$ of the wake centerline, for free-stream wind speeds of 9 ± 1 m/s. The plot shows the measured data and the data from the three wake models. Whiskers represents one standard deviation from the mean of the measured data. The left side of the 8-10 wake case is missing due to few data points.

The normalized power for the four remaining wake cases, shown in Figure 21, are characterized by more uncertainty than the previous plots in Figure 20. The wake region is also seen to be more asymmetrical. Especially in wake case '14-4', the measurement does not agree with the modeled predictions at the right side of the wake. Note that the two figures (21 and 22) have a different range on the y-axis. The standard deviation of the measured data is varying. In some wake cases, like case '1-5', a low deviation is observed

through the entire wake region. While in some cases, like '3-7', the standard deviation varies across the region. Last, there are several wake cases where the standard deviation is very high. In only a few wake cases does the normalized power converge to unity outside the wake. In most of the cases, the no-wake normalized power does not have the same value at the two sides of the wake.

From these power deficit profiles, it is not that easy to get a clear grasp on how accurate the models are. Regarding the peak of the wake, i.e. the wake centerline, Figure 22 shows the accuracy of the three wake models presented as a boxplot.
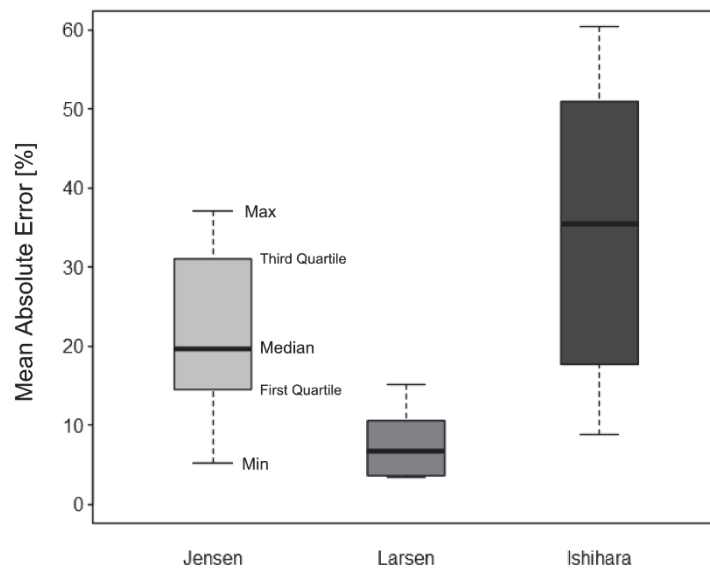
Figure 22. Mean absolute error of the three wake models compared to the measured values at the wake centerline ± 1°, for free-stream wind speeds of 9 ± 1 m/s, using all eight wake cases.

As can be seen in the figure above, there are significant differences in the accuracy of the models regarding the peak of the wake. The Larsen model is by far the most accurate, with a mean absolute error of 7 % and a maximum error of 15 %. The Jensen model has a mean absolute error of 21 % and a maximum error of 37 %. Finally, the Ishihara model performs worst, with a mean absolute error of 34 % and a maximum error of 60 %.

To see if the models are over- or under predicting, Figure 23 shows the mean error of the wake centerline. Both the Jensen- and Ishihara model are overestimating the wake loss at the centerline, while the Larsen model is seen both over- and underestimating.
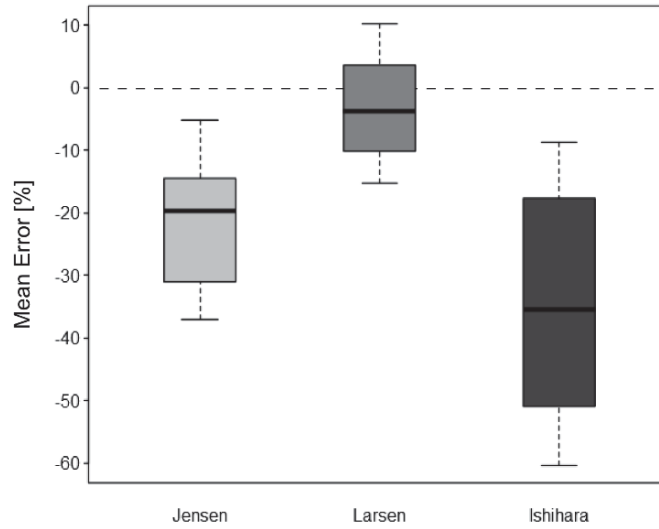
Figure 23. Mean error of the three wake models compared to the measured values at the wake centerline ± 1°, for free-stream wind speeds of 9 ± 1 m/s, using all eight wake cases.

To see how the three models predict the power deficit at the wake centerline for other speed intervals than the previously tested 9 ± 1 m/s interval, the normalized power deficit versus the free stream wind speed is plotted for two of the wake cases in Figure 24 below. Although there are some variation between the two plots, the measurements and the output of the three wake models show the same trend. The wake models error is almost constant throughout the wind speed interval.
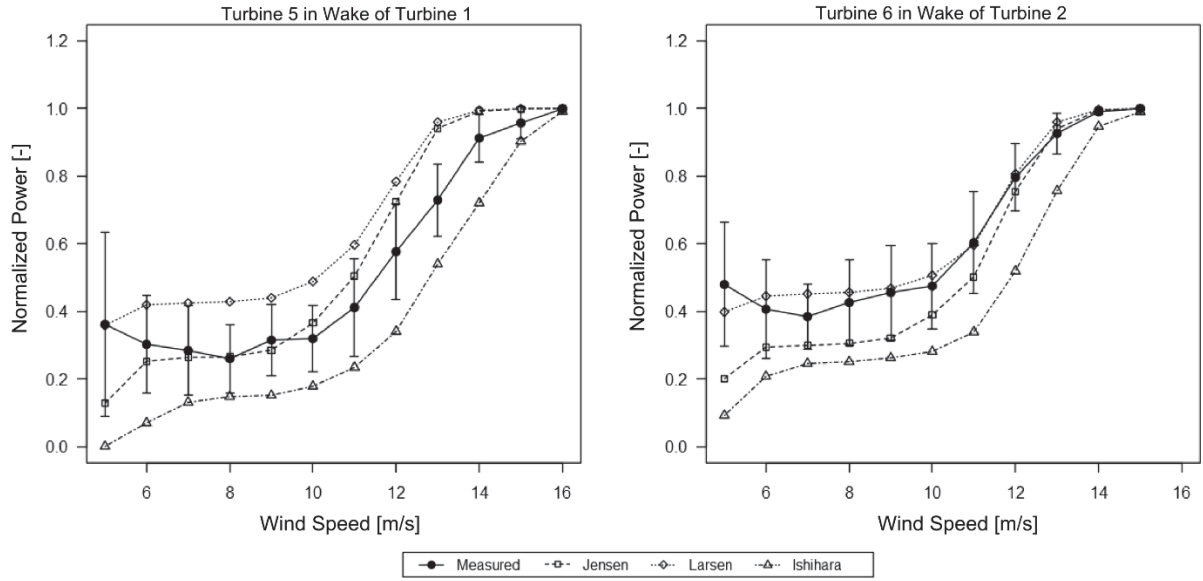
Figure 24. The measurements and the three wake models prediction of the normalized power deficit at the wake centerline ± 1° for a broad interval of wind speeds. Whiskers represents one standard deviation from the mean of the measured data.

The Larsen and Jensen model are in wake case '1-5' seen to reach unity before the measurements. In these cases, the mentioned models will predict a no-energy-loss wake situation (both turbines are operating at rated power) in situations where the measurements dictate an energy loss, resulting in an underestimation of the energy loss at these speeds. The Ishihara model, on the other hand, overestimating the centerline power deficit for the entire wind speed interval. An overestimation of the energy loss at the wake centerline follows. At low free stream wind speeds (<7 m/s, but varying) the measurements behave widely different then what the wake models assume. Instead of an expected sharp increase in the normalized power deficit, the measurements instead show a reduced deficit and a high standard deviation. It is also apparent from the plots that the Jensen model, from around a free stream wind speed of 9 m/s, starts to predict an increased rate of wake recovery with increasing wind speeds. This rate is higher than both the rate seen in the measurements and the other wake models for the same wind interval.
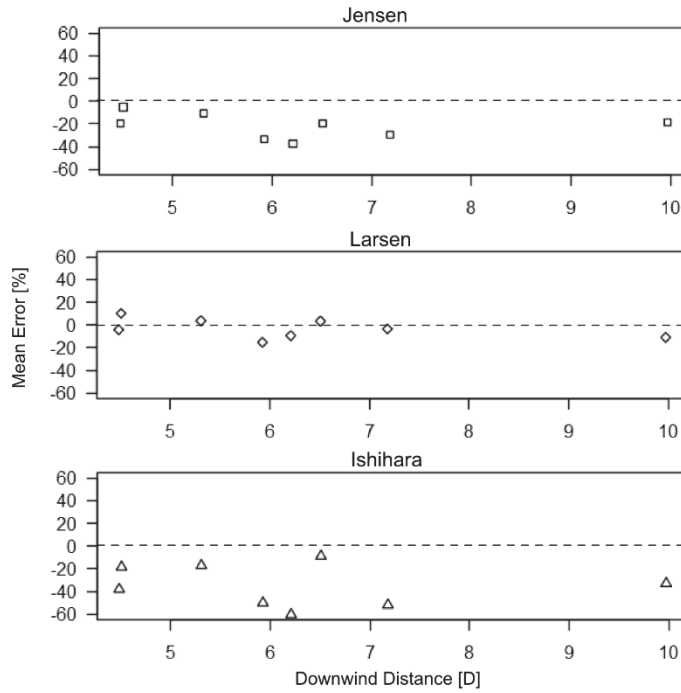
Figure 25. The mean error of the model predictions of the normalized power at the wake centerline ± 1° versus the distance between the turbines.

There is no clear trend in the accuracy of the models regarding the downstream distance, as seen in Figure 25. In wake cases where the Ishihara model performs badly, the Jensen model is likely to as well, and vice versa.

Large differences regarding the wake models prediction of the wake width are observed. As previously seen (Figure 20 and Figure 21), some of the wake cases show a more distinct "U"-shape than others. Due to this, only four of the wake cases are investigated regarding the wake width. In three of four cases, The Jensen model agrees well with the observed wake width, matching the wake width perfectly in one case, and with a mean absolute error of 6.8 %. The Larsen model overestimates the wake width in all cases (with an almost constant offset) with a mean absolute error of 22.0 %. Finally, the Ishihara model also shows decent results, with a mean absolute error of 10.5 %.
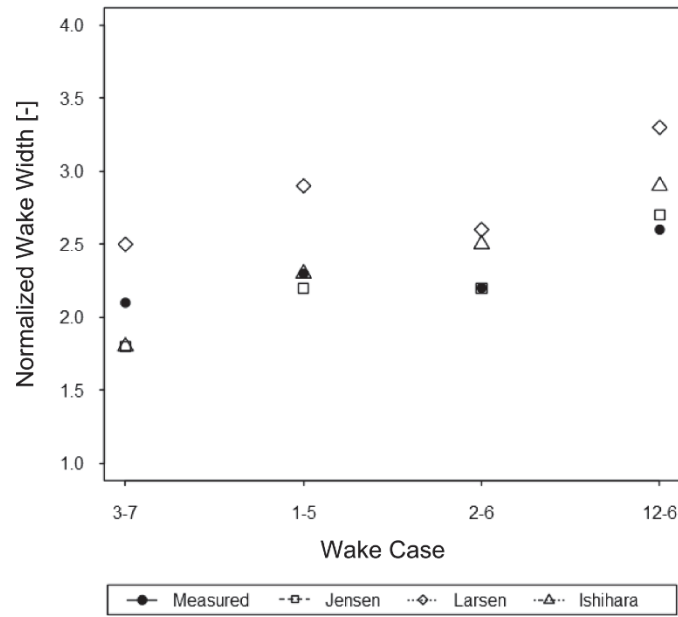
Figure 26. The normalized wake width for four wake cases. The wake is normalized to the rotor diameter of the turbine in front.

An estimation of the energy loss in the wake is done for three wake cases: '1-5', '2-6' and '3-7'. Large differences in the accuracy of the predicted energy loss in the wake are found. In two of the wake cases ('1-5' and '2-6'), all the wake models underestimate the wake loss, while it is overestimates in the last. Table 2 lists the error of the modeled energy loss in the wake for each wake model compared to the measurements.

Table 2. The error of the modeled energy loss in the wake for each wake model compared to measurements, for both uncorrected and corrected cases.

		Jensen model	**Larsen model**	**Ishihara model**
'1-5'	*Uncorrected*	-51.0 %	-46.2 %	-41.7 %
	Corrected	-24.9 %	-34. 8 %	-20.7 %
'2-6'	*Uncorrected*	-15.5 %	-27.1 %	-4.1 %
	Corrected	-1.8 %	-18.3 %	-2.3 %
'3-7'	*Uncorrected*	40.2 %	12.7 %	58.0 %
	Corrected	4.9 %	17.6 %	6.7 %
Mean abs. error	*Uncorrected*	36 %	29 %	35 %
	Corrected	11 %	24 %	10 %

For the uncorrected cases, the Ishihara model is the most accurate in two of three cases ('1-5' and '2-6'), even though the Larsen model is the most accurate with regard to the mean

absolute error (29 %) since the Ishihara model is highly inaccurate in case '3-7'. The Jensen- and Ishihara model proves equally accurate, with a mean absolute error of 36 and 35 % respectively. The energy loss with the correction procedure proves more accurate for all but one instance (Larsen model forthe wake case '3-7'). Now, the Larsen model proves to be most inaccurate (mean absolute error of 24 %), while the Jensen- and Ishihara performs much better, and again almost equally with mean absolute errors of 11 and 10 % respectively). For the Larsen model, there is only a small improvement from the uncorrected to the corrected error, while both the Jensen- and Larsen model shows a large improvement.
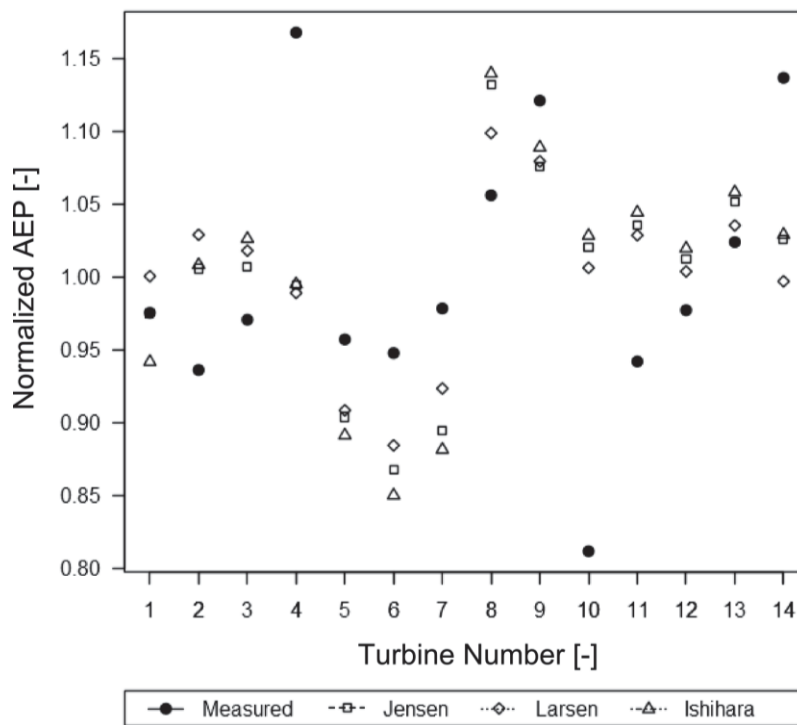

Figure 27. The normalized annual energy production for each turbine. The measurements are compared to the simulated data (for each of the three wake models).

The plot of the normalized AEP (Figure 27) for each turbine shows that the simulations to some degree capture the trend in the measurements. There are varying degree of scatter between the different wake models. In some cases, like with turbine 4 or 9, they show little variation, while for turbine 1, 6, 7 and 8, they deviate from each other. At turbine 4, 10 and 14, the measurements differs from the simulated values. It is quite interesting that the simulation capture the high producing turbines 8 and 9. From this comparison, the Larsen model performs best, then the Jensen model and finally the Ishihara model.

4.1   ACTUATOR DISC

The actuator disc approach in WindSim provided accurate results for the one wake case it was tested on (wake case '1-5'). Figure 28 below illustrates the result of a WindSim simulation, showing the 3D speed scalar for the wind field around turbine 1 (in front) and turbine 5 (in the wake) for a wind direction of 270°.
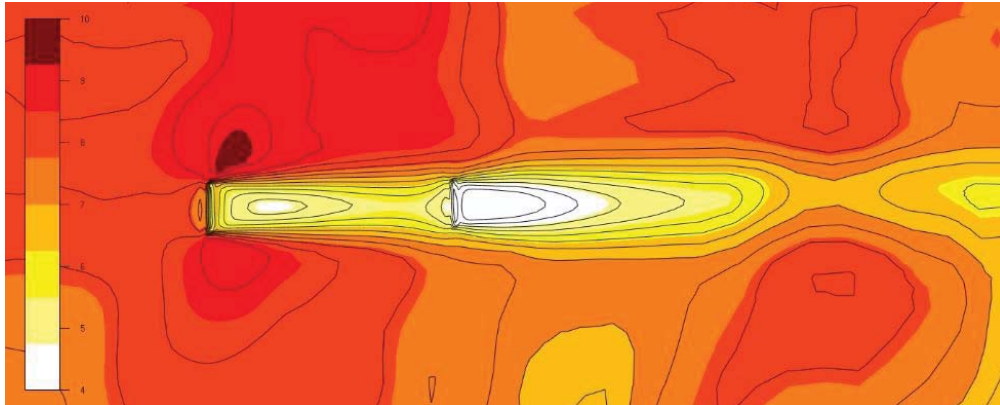
Figure 28. The result of the actuator disc approach for the wake case 1-5, for a wind direction of 270°. The wind speed legend is shown on the left.

The velocity deficit in the wake was accurately modeled as seen in Figure 29 below. A slight overestimation the wind velocity at turbine five is present. At a free-stream wind speed of around 11 m/s, the point where the simulation disagrees most with the measurements, the uncertainty in the measured data is high.
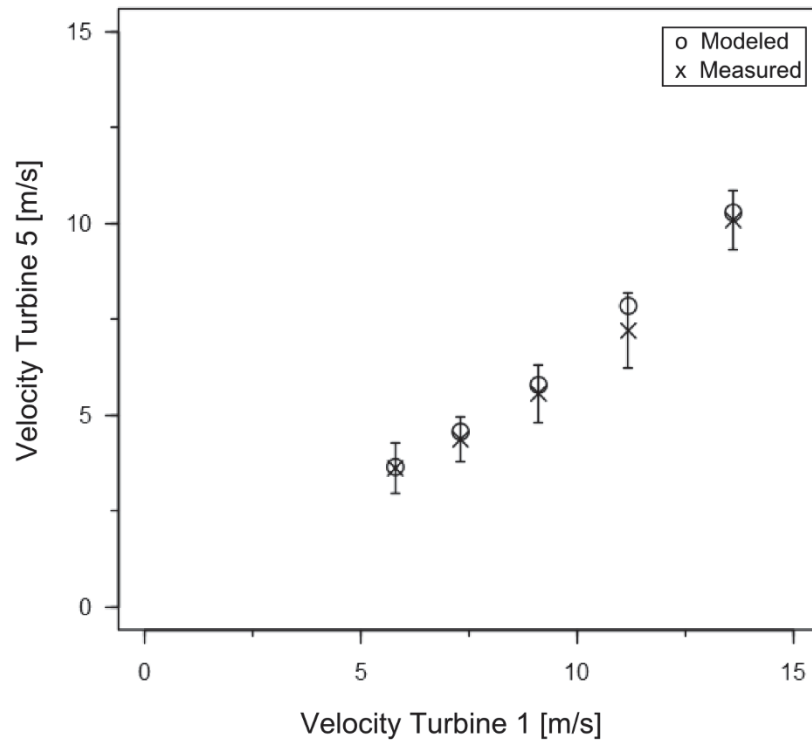
Figure 29. Plot of both the modeled and measured values for the wind speed at turbine 5 as a function of wind speed at turbine 1 for a wind direction of 270°. Whiskers indicate one standard deviation from the mean of the measured data.

5 DISCUSSION

In order to validate three kinematic wake models, namely the Jensen-, Larsen-, and Ishihara model, the CFD-based WindSim software was used together with data from an onshore wind farm in Norway positioned in complex terrain. A set of tests were performed to test the accuracy of the wake models. Of the three models investigated, the Larsen model proved to be the most accurate regarding the power deficit in the wake, although it showed some tendencies to underestimate the deficit. Both the Jensen- and Ishihara-model overestimates the wake deficits throughout the wake region, although the Jensen model was closer to the measurements than the Ishihara model. The same applies for the wake centerline; the Larsen model is found to be the most accurate of the three models. The Jensen model is to some degree overestimating the normalized power deficit, while the Ishihara model largely overestimates the deficit at the centerline. Gaumond et al. (2012) found the Larsen model slightly underestimating the power deficit in single-wake cases at both Horns Rev- and Lillgrund wind farm. The Jensen model showed a good fit to the measurements. But, those were offshore. In the study by Duckworth and Barthelmie (2008), using data from two onshore wind farms, both the Larsen- and Jensen model (in the study referred to as the Katic model) show varying performance. The Ishihara model is known to over predict the wake loss, as reported in amongst others Pillai et al. (2014) and Crasto et al. (2011).

Since the Ishihara-model is newer than the other models and therefore not implemented in that many programs, there are few field studies where it is tested, implying that it is difficult to find other work for which to compare the results obtained in this thesis. The Larsen- and Jensen models on the other hand have been around for a while and are tested in many studies.

Regarding the normalized power deficit at the wake centerline versus the free stream wind speed, all wake models follow the trend in the measurements, but with clearly different magnitudes. The Larsen model - and to some degree the Jensen model- reaches a no-wake situation before the measurements, i.e. at a lower free-stream wind speed. The Ishihara on the other hand reaches a no-wake situation after the measurements. This implies the Larsen model, and in some cases the Jensen model, will underestimate the energy loss, especially at higher wind speeds. On the other hand, the Ishihara model overestimates the centerline wake loss for all wind speeds.

Regarding the width of the wake, there were significant differences between the wake models. Both the Jensen- and Ishihara model provided an accurate prediction of the wake width, while the Larsen model is seen to overestimate the wake width in all the investigated cases. In Tong et al. (2012) the Larsen model is seen to predict a larger wake width than the Jensen- and Ishihara model. Also Renkema (2007) finds the Larsen model overestimating the wake width, while the Jensen provides a good fit. Both the Larsen- and Jensen model predict the wake width very accurately in Gaumond et al. (2012), but again, that was offshore. In the master's thesis by Borràs (2015), all the three wake models are found to overestimate the wake width obtained from measurements at Horns Rev. The Jensen model is found to be most accurate.

Because of the uneven speed-up at the turbine locations due to the terrain, leading to an asymmetrical wake profile, only four wake cases could be investigated with regard to the wake width. With so few cases, it is hard to identify trends with confidence. Another factor is the small separation of the cases investigated with regard to the wake distance, ranging from only 5.1 to 6.5 D, leaving us without information on how the wake width behaves outside this narrow region. However, the in-between distance of turbines in most onshore wind farms lies inside this distance-interval, so it is certainly an important region.

Large differences in the wake models estimation of the energy loss in wake is found. Without the correction procedure, the Larsen model is the most accurate, although all models show a high degree of scatter. Employing the correction, the Larsen suddenly proves to be the most inaccurate, while the Jensen- and Ishihara model give better results. Renkema (2007) found large differences between the Larsen model and the Jensen model for the energy loss in the wake.

The reason for why the wake models still underestimate the energy loss, even though previous results indicate that the wake loss is overestimated, is because of incorrect estimation of the wind speed by the CFD simulation. The wind speed, and thereby the power production, is overestimated, leading to an underestimation of the energy loss in the wake.

The comparison of the measured and simulated AEP for each turbine (through a normalization procedure) showed that the simulation captures the difference between the turbines to some extent. It is hard to draw any real results out of this comparison because of the employed procedure. The measured normalized AEP of turbine 4, 10 and 14 deviated significantly from the modeled values. Both turbine 4 and 14 perform much better than the simulation expects. It is presumed that these two turbines perform well due to

increased wind speeds caused by the mountains in the north. It is evident that the simulation captures this effect inadequately. Turbine 10 performed worse than expected by the simulation. It is placed low in the terrain and the terrain data might overestimate the elevation at the point, i.e. that the turbine is placed higher above the ground in the simulation than what it really is (M. Homola 2015, pers. comm.). This might have caused the simulation's overestimation. It is possible that this effect was increased by the smoothing procedure.

The actuator disc approach provided good agreement with measurements, although only one wake case was tested, and for only one wind direction. It is more computational demanding than the standard simulation in WindSim, and it is expected to treat the interaction between the wake and the terrain with more precision (Gravdahl et al. 2012). Wind tunnel tests have shown that the actuator disk method proves accurate for far-wake conditions (Kalvig et al. 2012).

Uncertainty in the measurements, as is the nature of field data, complicated the validation procedure because the nature is not steady state as the simulations. Even though the measurements are averaged over a ten minute-interval, they do show a fluctuating behavior. The averaging of the measurements is of course necessary to reduce the amount of data. Holes in the datasets caused some trouble, as fewer measurements were available for the validation procedure.

As mentioned in the introduction, complex terrain has always been a challenge for the wind energy community. It still is, but CFD models may change this as they should be capable of accurately describe the wind field over complex terrain. But the CFD models still need adequate amount of input data, i.e. high quality measurements of the wind, and enough computer capacity. In flat terrain or offshore, where the wind field can be assumed homogenous over the whole area, there shouldn't be the need for more than one mast with measurements at different height to measure the wind shear and atmospheric stability. In complex terrain however, one measurement mast proves to be inadequate. Politis et al. (2012) emphasizes the need for "multimast campaigns" in such terrain. This of course increases the costs. The use of LIDAR-measurements can make modeling in complex terrain easier. Data from more points within the area of interest will be available, and it is also possible to employ measuring devices within an existing farm. This would be of great interest for the use in validation studies (Kumer).

Since the measurement mast often are substantially lower than the hub height of a turbine, so also at Nygårdsfjellet, the wind speed at hub height needs to be estimated from

the simulated wind shear. Due to some unknown problems with the anemometers located at both 20 and 30 meters on the measurement mast, only the measurements recorded at 40 meters were used. This of course creates uncertainty in the wind speed transfer from the met mast and upwards, as the wind shear is unknown. The study found more spread in the measured wind directions at the mast then the measured yaw directions at the turbines. It can be that the wind is more directionally stable at higher elevations, or it can be that the turbine settings causes a more stationary yaw direction. Either way, since the simulations use the wind direction frequency measured at the mast, the modeled yaw directions of the turbines show a much wider spread than the measurements do.

The CFD model assumes a neutral stratification of the atmosphere, which many times are a bad assumption. It must be expected that the stratification is in a stable state at Nygårdsfjellet especially during the winter. This is certainly something to look into, as wake losses are reported to be higher when the atmosphere is stable, for example in Hansen et al. (2012).

The problems encountered regarding the shift of the measured wake compared to the modeled wake, although it was corrected for by a simple procedure, indicates that something are wrong. The problem might come from the measurements or from the simulation, or both. This was also discussed in Politis et al. (2012), where four different reasons were pinpointed. All of them are plausible explanation for the observed shift. Measurements from some of the turbines at Nygårdsfjellet shows yaw alignments that cannot be attributed to terrain effects alone. This indicates that the turbine either operate under yaw misalignment or that there is a static recording error (Nordkraft informs that the instruments are not calibrated (M. Homola 2015, pers. comm.)). Uncertainty of the measured data are also plausible, both regarding the measurements from the met mast and the turbines. Although tests indicated that grid independence was achieved, it is not thereby said that the simulation is a good representation of the real world. CFD modeling requires a lot of expertise and experience. Due to computational limits, the simulations were not performed with the desired number of cells. The simulations was also performed with too few layers in the vertical direction.

The complex terrain, and its effect on the wind field, increases the uncertainty in the modeling. A source of modeling error might come from the use of the manufacturer's power curve without adjustments, i.e. without adapting them to the local conditions (Politis et al. 2012). There are some differences in how the measurements from the turbines fits the

manufacturer's power curve, as seen in appendix B. And thereby it follows that using the same power curve for each turbine ultimately leads to errors.

The method of just shifting the wake centerline with a fixed value was unavoidable in order to compare the simulated data to the measurements. Calculations show that this offset is not static, as it changes somewhat with the wind speed. Since the methods is employed in the 9 ± 1 m/s-interval, this implies that the method of adjusting the yaw-measurements with a fixed value leads to errors for all results obtained outside this speed interval.

The wake-wake interaction was not investigated in this thesis, but it could certainly be of interest. It is complicated because the turbine first of all are not positioned in straight lines, but also because of the presence of other issues remarked in this thesis.

Since this thesis was set to validate the kinematic wake models, and not the CFD simulation in itself, the successfulness of this study depended on satisfying simulations. As this was not accomplished, the modeled data had to be corrected, thus decoupling the output of the simulation and the wake models. This made it possible to carry on with the validation procedure. It is of course not a desired approach, but it proved to be necessary.

This study has not investigated how different settings for important factors such as the turbulence intensity and wake decay constants influences the results, using only the default settings in WindSim. It is possible that changes in these parameters will have a big impact on the accuracy of three wake models. Borràs (2015) shows that the output of the three wake models are highly dependent on the choice of values. This was out of the scope of this master's thesis, but is certainly something that deserves further investigation.

6 CONCLUSION

Significant differences in the prediction capabilities of the three wake models were found. Overall, findings indicated that the Larsen model performed best, although it constantly overestimated the width of the wake and showed tendencies to underestimate the energy loss in the wake. The Jensen model proved reasonable accurate while the Ishihara model showed clear signs of overestimating the energy loss. But no clear-cut conclusion can be drawn on which wake model is the most accurate, due to both terrain-related issues that complicated the validation procedure and uncertainty in the measurements. Even if one could say which is the best, it wouldn't necessarily dictate which model is the most accurate at another site. This is the downside of a field study, not knowing the external validity. The findings are always, at least to some degree, site-dependent. It must be emphasized (like in Politis et al. (2012)) that validation studies in complex terrain require more than one measuring point, either in the form of multiple masts or LIDAR-measurements. Also, the need for a fine grid, requiring powerful computers, is absolutely necessary in complex terrain. Future work can include further refined CFD-simulations, possible also testing the actuator disc-approach for more wake cases. Also interesting would be to employ LIDAR-devices in order to get better measurements of the wind field and the wake itself. The effect of changing different wake model parameters should also be investigated.

REFERENCES

Ainslie, J. F. (1988). Calculating the flowfield in the wake of wind turbines. *Journal of Wind Engineering and Industrial Aerodynamics*, 27 (1-3): 213-224.

Barthelmie, R. J., Frandsen, S. T., Rathmann, O., Hansen, K. S., Politis, E. S., Prospathopoulos, J., Cabezón Martínez, D., Rados, K., Van Der Pijl, S. & Schepers, J. (2008). Flow and wakes in large wind farms in complex terrain and offshore.

Barthelmie, R. J., Pryor, S., Frandsen, S. T., Hansen, K. S., Schepers, J., Rados, K., Schlez, W., Neubert, A., Jensen, L. & Neckelmann, S. (2010). Quantifying the impact of wind turbine wakes on power output at offshore wind farms. *Journal of Atmospheric and Oceanic Technology*, 27 (8): 1302-1317.

Berge, E., Gravdahl, A. R., Schelling, J., Tallhaug, L. & Undheim, O. (2006). Wind in complex terrain. A comparison of WAsP and two CFD-models. *Proceedings EWEC. Año*.

Borràs Morales, J. (2015). *Park optimization and wake interaction study at Bockstigen offshore wind power plant*: Uppsala University, Dept. of Earth Sciences, Campus Gotland.

Crasto, G., Castellani, F., Gravdahl, A. R. & Piccioni, E. (2011). Offshore wind power prediction through CFD simulation and the actuator disc model. *EWEA ANNUAL EVENT*.

Crasto, G., Gravdahl, A. R., Castellani, F. & Piccioni, E. (2012). Wake Modeling with the Actuator Disc Concept. *Energy Procedia*, 24 (0): 385-392.

Crespo, A., Hernandez, J. & Frandsen, S. (1999). Survey of modelling methods for wind turbine wakes and wind farms. *Wind energy*, 2 (1): 1-24.

De Souza, A. (2005). *How to–Understand Computational Fluid Dynamics Jargon*: Published.

Duckworth, A. & Barthelmie, R. (2008). Investigation and validation of wind turbine wake models. *Wind Engineering*, 32 (5): 459-475.

Elliott, D. (1991). Status of wake and array loss research: Pacific Northwest Lab., Richland, WA (United States).

European Commission. (2014). *A policy framework for climate and energy in the period from 2020 to 2030*.

European Parliament, C. o. t. E. U. (2009). Directive 2009/28/EC of the European Parliament and of the Council of 23 April 2009 on the promotion of the use of energy from renewable sources and amending and subsequently repealing Directives 2001/77/EC and 2003/30/EC.

EWEA. (2015). Wind in power: 2014 European statistics.

Frandsen, S. T., Chacón, L., Crespo, A., Enevoldsen, P., Gómez-Elvira, R., Hernández, J., Højstrup, J., Manuel, F. & Thomsen, K. (1996). *Measurements on and modelling of offshore wind farms*.

Gaumond, M., Réthoré, P.-E., Bechmann, A., Ott, S., Larsen, G. C., Peña, A. & Hansen, K. S.
(2012). *Benchmarking of wind turbine wake models in large offshore wind farms*.
Proceedings of the Science of Making Torque from Wind Conference.

Gravdahl, A. R., Crasto, G., Castellani, F. & Piccioni, E. (2012). *Wake modeling with the Actuator
Disc concept*: Sintef.

Hansen, K. S., Barthelmie, R. J., Jensen, L. E. & Sommer, A. (2012). The impact of turbulence
intensity and atmospheric stability on power deficits due to wind turbine wakes at Horns
Rev wind farm. *Wind Energy*, 15 (1): 183-196.

Homola , M. C., Nicklasson, P. J. & Sundsbø, P. A. (2009). *Two years of icing monitoring at
Nygårdsfjellet Wind Park*. IWAIS XIII, Andermatt, Switzerland.

Ishihara, T., Yamaguchi, A. & Fujino, Y. (2004). Development of a new wake model based on a
wind tunnel experiment. *Global wind power*.

Jensen, N. O. (1983). *A note on wind generator interaction*. Risø-M-2411. Risø, Denmark.

Kalvig, S. M., Manger, E. & Hjertager, B. (2012). *Comparing different CFD wind turbine
modelling approaches with wind tunnel measurements*. The Science of Making Torque
from Wind, Oldenburg, Germany.

Katic, I., Højstrup, J. & Jensen, N. O. (1987). *A Simple Model for Cluster Efficiency*. EWEC'86,
Rome.

Kumer, V. Lidar Measurements for Wind Energy Applications. Available at:
http://www.norcowe.no/doc//Documnets%20for%20web/LIDAR%20measurements%20fo
r%20wind%20energy%20applications.pdf. (accessed: 20/04)

Landberg, L. (2012). Wind Resources and Wakes. Stockholm: Elforsk.

Larsen, G. C. (1988). A Simple Wake Calculation Procedure. Risø-M-2860.

Lissaman, P. B. S. (1979). Energy effectiveness of arbitrary arrays of wind turbines. *Journal of
Energy*, 3 (6): 323-328.

Lissaman, P. B. S. (1994). Wind Turbine Airfoils and Rotor Wakes. In Spera, D. A. (ed.) *Wind
turbine technology: fundamental concepts of wind turbine engineering*, p. 638 s. : ill. New
York: ASME Press.

Magnusson, M. & Smedman, A. S. (1999). Air flow behind wind turbines. *Journal of Wind
Engineering and Industrial Aerodynamics*, 80 (1–2): 169-189.

Moskalenko, N., Rudion, K. & Orths, A. (2010). *Study of wake effects for offshore wind farm
planning*. Modern Electric Power Systems (MEPS), 2010 Proceedings of the International
Symposium: IEEE. 1-7 pp.

Nordkraft. *Vindforhold*. Available at: http://www.nordkraftvind.no/no/Vare-
prosjekter/Nygardsfjellet-trinn-I/Vindforhold/ (accessed: 20/03).

Pillai, A. C., Chick, J. & de Laleu, V. (2014). *Modelling Wind Turbine Wakes at Middelgrunden
Wind Farm*. EWEA, Barcelona, Spain.

Politis, E. S., Prospathopoulos, J., Cabezon, D., Hansen, K. S., Chaviaropoulos, P. K. & Barthelmie, R. J. (2012). Modeling wake effects in large wind farms in complex terrain: the problem, the methods and the issues. *Wind Energy*, 15 (1): 161-182.

Rados, K., Prospathopoulos, J., Stefanatos, N., Politis, E., Chaviaropoulos, P. & Zervos, A. (2009). *CFD modeling issues of wind turbine wakes under stable atmospheric conditions*. Europeen Wind Energy Conference & Exhibition Proceedings, Marseille, France.

Renkema, D. J. (2007). *Validation of wind turbine wake models: Using wind farm data and wind tunnel measurements*: Delft University of Technology, Faculty of Aerospace Engineering.

Rohatgi, J. & Barbezier, G. (1999). Wind turbulence and atmospheric stability—their effect on wind turbine output. *Renewable energy*, 16 (1): 908-911.

Sanderse, B. (2009). Aerodynamics of wind turbine wakes. *Energy Research Center of the Netherlands (ECN), ECN-E–09-016, Petten, The Netherlands, Tech. Rep*.

Schlez, W. & Neubert, A. (2009). *New developments in large wind farm modelling*. Proceedings of the European Wind Energy Association Conference.

Thomsen, K. & Sørensen, P. (1999). Fatigue loads for wind turbines operating in wakes. *Journal of Wind Engineering and Industrial Aerodynamics*, 80 (1): 121-136.

Tong, W., Chowdhury, S., Zhang, J. & Messac, A. (2012). Impact of Different Wake Models on the Estimation of Wind Farm Power Generation.

Vermeer, L. J., Sorensen, J. N. & Crespo, A. (2003). Wind turbine wake aerodynamics. *Progress in Aerospace Sciences*, 39 (6-7): 467-510.

WindSim. (2009). Wind Resources. Available at: https://www.windsim.com/ws_docs/ModuleDescriptions/WindResources2.html (accessed: 20/03/2015).

WWEA. (2014). Half-year Report 2014.

APPENDIX A: SIMULATED WAKE VELOCITY DEFICITS

Output from the WindSim-simulations showing the predicted wake velocity deficits by each wake model.
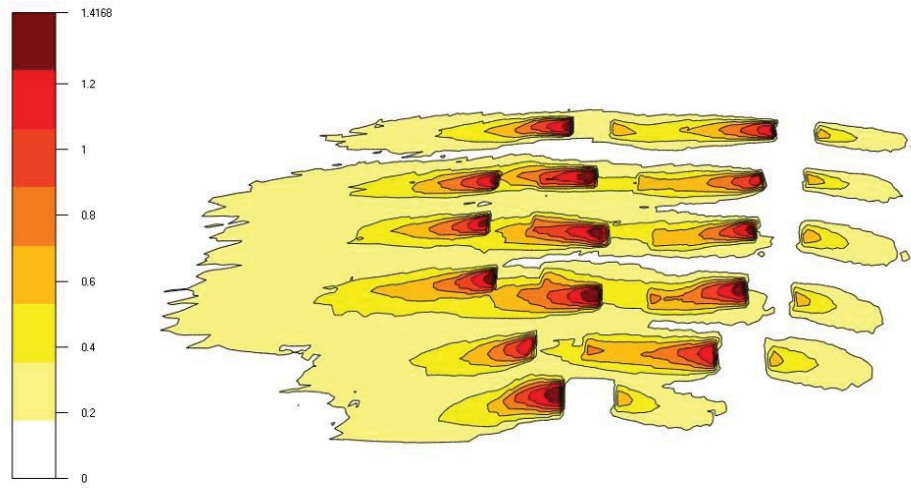
Jensen model
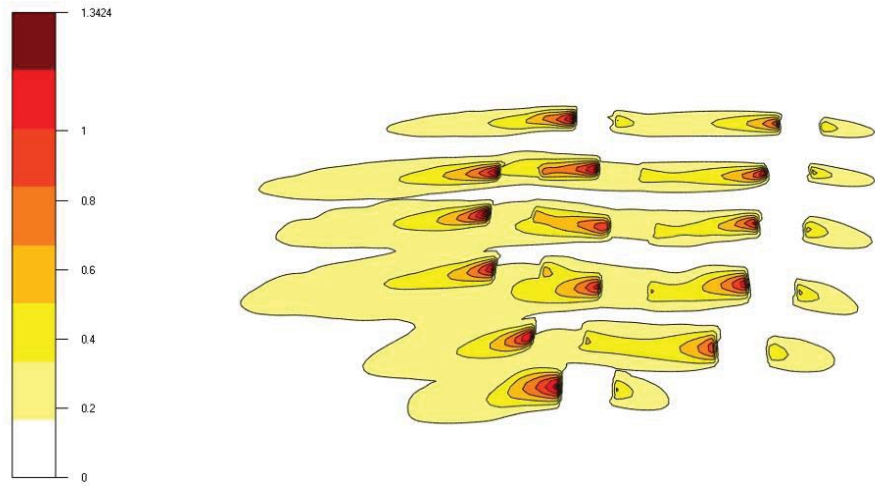
Larsen model
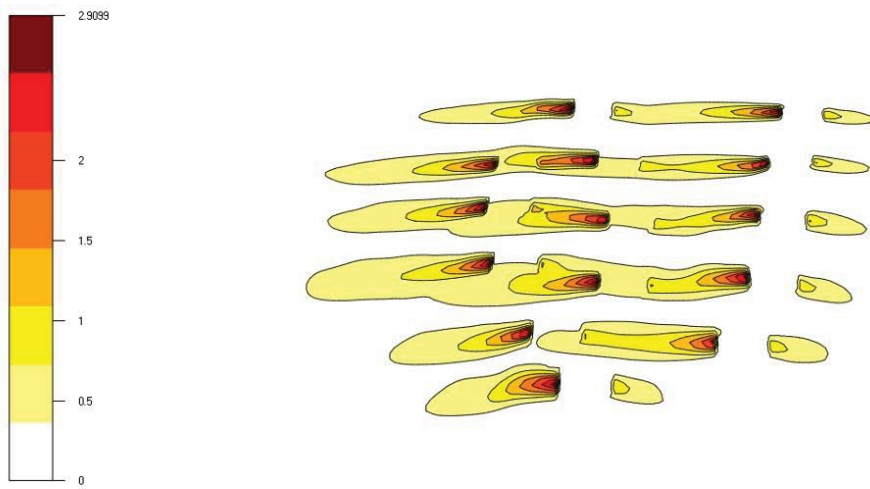
Ishihara model
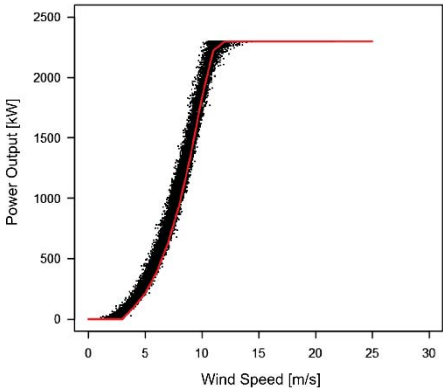
APPENDIX B: POWER CURVES

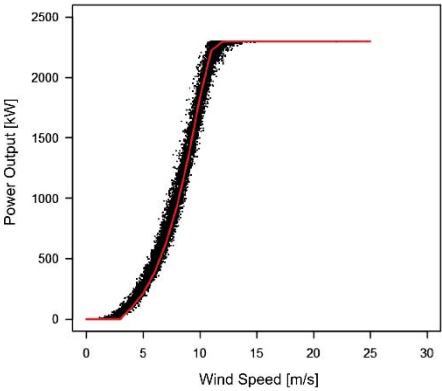The manufacturer's power curve for the Siemens SWT 2.3 MW 93 (shown in red) versus the measured data (shown in black) for each turbine.
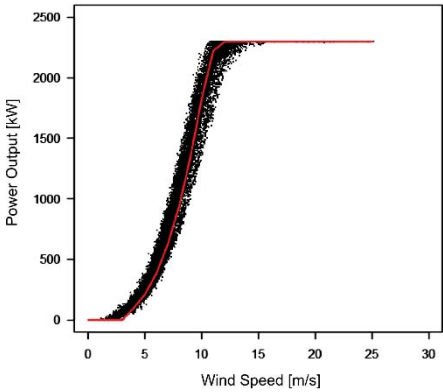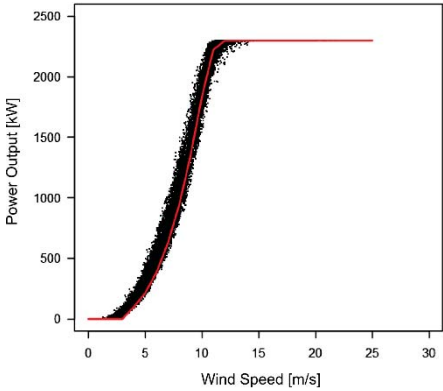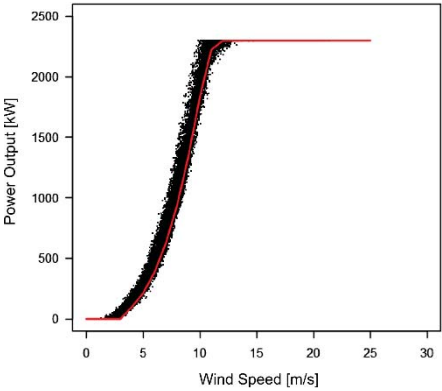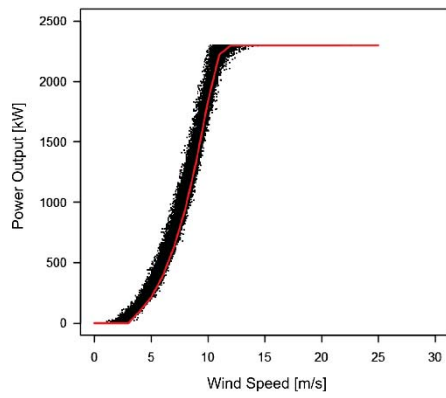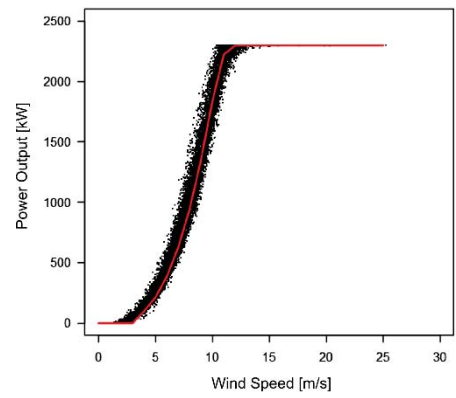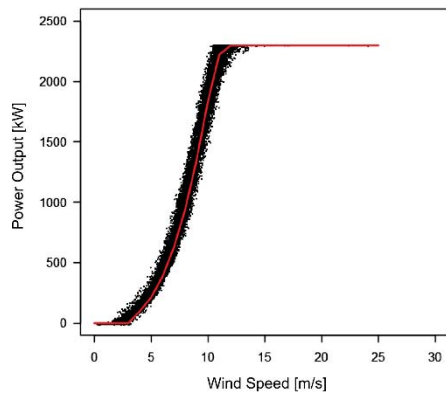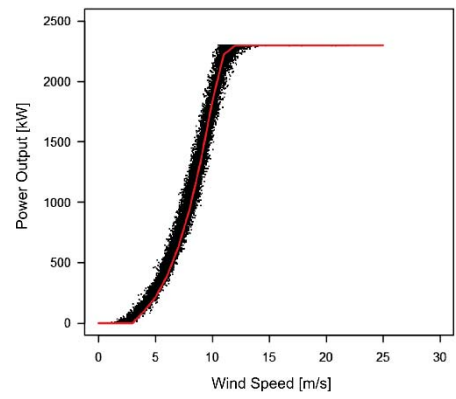

Turbine1
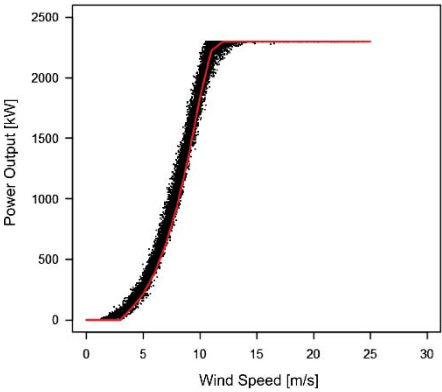
Turbine2

Turbine 3

Turbine 4

Turbine 5

Turbine 6

Turbine 7

Turbine 8

Turbine 9

Turbine 10
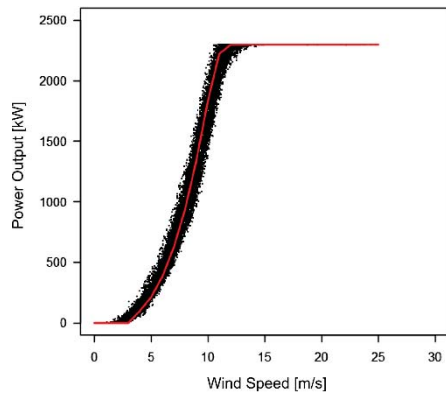
Turbine 11

Turbine 12

Turbine 13

Turbine 14